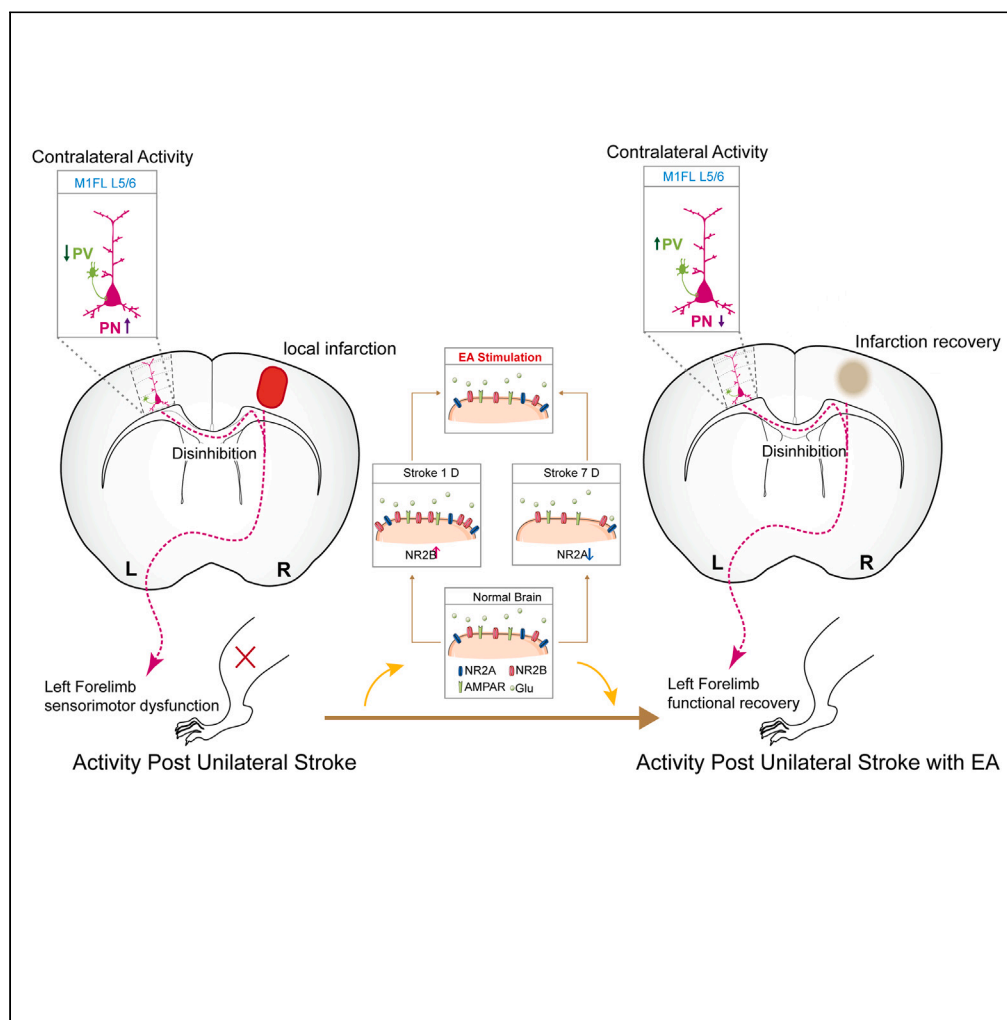**Article**

Pyramidal and parvalbumin neurons modulate the process of electroacupuncture stimulation for stroke rehabilitation

Xiaorong Tang, Jiahui Shi, Shumin Lin, ..., Chunzhi Tang, Nenggui Xu, Lulu Yao

ngxu8018@163.com (N.X.)
yaolulu@gzucm.edu.cn (L.Y.)

Highlights

Electroacupuncture improved sensorimotor function following ischemic stroke

Electroacupuncture regulated disturbed neuronal activity in the contralateral M1FL

NMDARs contributed to the EA-mediated regulation of disturbed neuronal activity

Disturbed neuronal activity in the contralateral M1FL due to attenuated inter-inhibition from ipsilateral region

iScience

Article

Pyramidal and parvalbumin neurons modulate the process of electroacupuncture stimulation for stroke rehabilitation

Xiaorong Tang,[1,5] Jiahui Shi,[1,5] Shumin Lin,[1,5] Zhiyin He,[1] Shuai Cui,[2,3] Wenhui Di,[1] Siyun Chen,[1] Junshang Wu,[1] Si Yuan,[1] Qiuping Ye,[1] Xiaoyun Yang,[1] Ying Shang,[1] Zhaoxiang Zhang,[4] Lin Wang,[1] Liming Lu,[1] Chunzhi Tang,[1] Nenggui Xu,[1,*] and Lulu Yao[1,6,*]

SUMMARY

Electroacupuncture (EA) stimulation has been shown to be beneficial in stroke rehabilitation; however, little is known about the neurological mechanism by which this peripheral stimulation approach treats for stroke. This study showed that both pyramidal and parvalbumin (PV) neuronal activity increased in the contralesional primary motor cortex forelimb motor area (M1FL) after ischemic stroke induced by focal unilateral occlusion in the M1FL. EA stimulation reduced pyramidal neuronal activity and increased PV neuronal activity. These results were obtained by a combination of fiber photometry recordings, *in vivo* and *in vitro* electrophysiological recordings, and immunofluorescence. Moreover, EA was found to regulate the expression/function of N-methyl-D-aspartate receptors (NMDARs) altered by stroke pathology. In summary, our findings suggest that EA could restore disturbed neuronal activity through the regulation of the activity of pyramidal and PV neurons. Furthermore, NMDARs we shown to play an important role in EA-mediated improvements in sensorimotor ability during stroke rehabilitation.

INTRODUCTION

Stroke is one of the leading causes of death and disability worldwide.[1] The global cost of stroke is over 721 billion dollars annually.[2] By 2030, stroke is estimated to cause up to 12 million deaths, with more than 200 million disability adjusted life years lost globally.[3] Of the stroke cases, ischemic stroke accounts for 88%, with unilateral stroke accounting for approximately 40%.[4] Although improvements in stroke management could increase survival, many patients with stroke would suffer from persistent neurological deficits such as dyskinesia, paresis, aphasia, apraxia, or neglect.[5] Recently, numerous efforts have been focused on the field of neurorehabilitation regarding the development of adjunct therapies to promote functional recovery after stroke, such as transcranial magnetic stimulation, theta-burst stimulation, transcranial electric stimulation, mirror image movement enabler, and robot-assisted rehabilitation devices.[6,7] In addition, acupuncture therapy has shown encouraging results in clinical research and meta-analyses on patients with stroke.[8,9] Furthermore, electroacupuncture (EA) stimulation may exert neuroprotective effects via activating the neurons near ischemic foci, alleviating glutamate excitotoxicity, enhancing cerebral blood flow, and regulating oxidative stress, inflammation, growth factors, and neuronal death signaling pathways following ischemic brain injury.[10–12] However, during the EA-mediated promotion of stroke rehabilitation, the role of neuronal activity in the bilateral hemisphere remains to be systematically explored.

Human functional imaging studies have identified a key role of the contralesional hemisphere during stroke recovery, which has been reported to be associated with enhanced neuronal activity in patients.[13,14] Both clinical and preclinical studies have suggested that an improvement in neuronal activity was associated with favorable recovery in both the contralesional and ipsilateral hemispheres.[15–17] Neuronal activity in the central nervous system (CNS) was attributed to the activity of pyramidal and inhibitory neurons, which constitute 80% and 20%, respectively, of the neurons in the cortical areas.[18] Pyramidal neurons are the principal excitatory neurons and serve as the core of cognitive function, sensory perception, and consciousness. Among the inhibitory neurons, parvalbumin (PV) neurons constitute approximately 40% of cortical interneurons and are known to innervate the axon initial segment of pyramidal neurons in a strategical region where the action potential is generated.[19] They primarily govern cortical pyramidal cells and play a

[1]South China Research Center for Acupuncture and Moxibustion, Medical College of Acu-Moxi and Rehabilitation, Guangzhou University of Chinese Medicine, Guangzhou 510006, China
[2]Research Institute of Acupuncture and Meridian, Anhui University of Chinese Medicine, Hefei 230000, Anhui Province, China
[3]College of Acupuncture and Moxibustion, Anhui University of Chinese Medicine, Hefei 230000, Anhui Province, China
[4]State Key Laboratory of Chemical Oncogenomics, Guangdong Provincial Key Laboratory of Chemical Genomics, Peking University, Shenzhen 518055, China
[5]These authors contributed equally
[6]Lead contact
*Correspondence: ngxu8018@163.com (N.X.), yaolulu@gzucm.edu.cn (L.Y.)
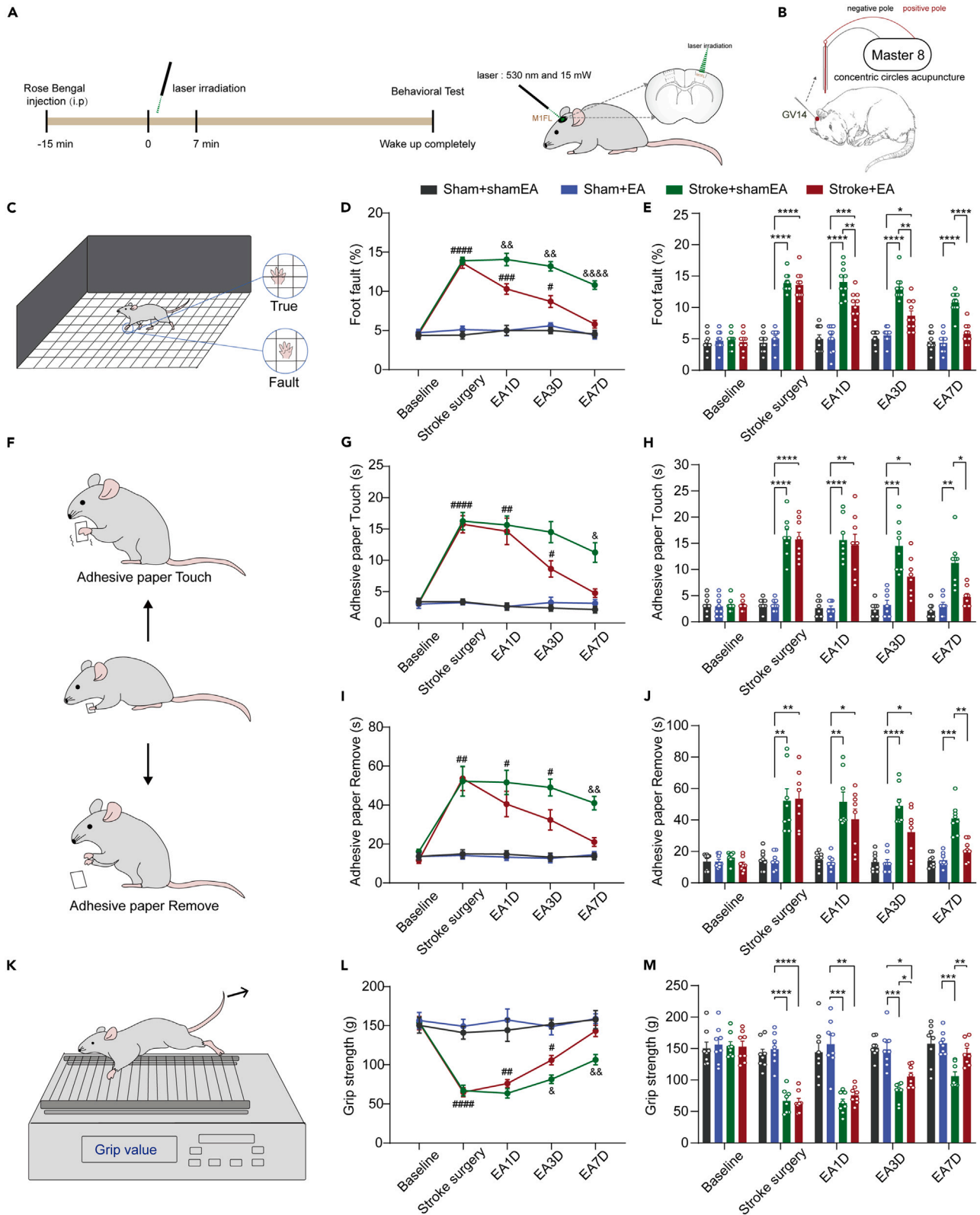https://doi.org/10.1016/j.isci.2024.109695

Figure 1. EA could restore M1FL infarction-induced forelimb dysfunction in mice

(A) Schematic of Photothrombotic model surgery.

(B) Schematic of EA stimulation. A concentric EA needle (φ 0.5 × 10 mm) was inserted at GV14 and EA stimulation was performed with the electric current of 1.0 mA and the frequency of 2 Hz.

(C) Schematic of Grid Walking Test. Foot fault rate was quantified by formula (foot faults/total steps * 100%) of the affected forelimb paw.

(D and E) EA stimulation rescues the increased of foot fault rate after stroke in mice. (n = 10 mice per group).

(F) Schematic of Adhesive Sticker Removal Test. Adhesive touch was recorded the time for mice to notice the adhesive paper on their affected forelimb paw. Adhesive remove was recorded the time for mice to remove the adhesive paper on their affected forelimb paw.

(G–J) EA stimulation rescue the increased of notice and remove the adhesive paper time after stroke in mice. (n = 8 mice per group).

(K) Schematic of Forelimb Grip Strength Test. Grip strength was recorded the grip value of mice forelimb paw by the Grip Tester.

(L and M) EA stimulation rescues the decreased of grip value after stroke in mice. (n = 8 mice per group). (D to M) *Two-way analysis of variance (ANOVA)* with *Tukey* post hoc test, *$p < 0.05$, **$p < 0.01$, ***$p < 0.001$, ****$p < 0.0001$. Stroke+EA vs. Sham+EA: ###$p < 0.001$, ##$p < 0.01$, #$p < 0.05$; Stroke+EA vs. Stroke+shamEA: &&$p < 0.01$, &$p < 0.05$. All data are represented by *mean± SEM*.

significant role in maintaining the finely tuned balance of excitation–inhibition within the brain.[20,21] Therefore, both pyramidal and PV neurons have been analyzed regarding their regulation of the excitability of the entire brain.[20,22]

Impaired motor function was reported to be related to the pathological alteration of pyramidal and PV neurons.[23,24] In the context of ischemic stroke, pyramidal neurons are not only involved in the downstream conduction of motor dominion, sending their axons downwards to the spinal cord to drive the muscles, but they also profoundly impact the contralesional homotopic brain area.[25] Simultaneously, loss of the inhibitory functional capacity within PV neurons may lead to a decrease in the control of pyramidal neuronal activity and a reduction in connectivity within larger brain networks.[26] Understanding the pathological changes of pyramidal and PV neurons is important in the stroke recovery. Therefore, unraveling the role of pyramidal and PV neurons during both the acute and recovery stages of stroke could strengthen our knowledge of EA-mediated improvements in stroke rehabilitation.

The N-methyl-D-aspartate receptor (NMDAR) is a glutamatergic neurotransmitter receptor that plays a critical role in physiological function and pathophysiological conditions, such as stroke and schizophrenia.[27,28] The NMDAR is a heterotetrameric complex with two glycine-binding GluN1 subunits and two glutamate-binding GluN2 subunits.[29] It was suggested that the NR2A subunit is related to better recovery following stroke, while the NR2B subunit is associated with worse recovery. The dual roles of NMDARs in neuronal survival and death may depend on the subcellular locations and subtypes of the receptors that are activated.[30] Therefore, this study aimed to investigate the function of NMDARs and the expression of different GluN2 subunits of NMDAR in EA-mediated stroke recovery.

In the study, in a mouse model of unilateral cortical stroke induced by photothrombotic surgery, we observed enhanced pyramidal neuronal activity and attenuated PV neuronal activity in the contralesional cortex both *in vivo* and *in vitro*. The important role of pyramidal and PV neurons during stroke recovery was further confirmed by chemogenetic manipulation. Furthermore, with a combination of electrophysiological recordings and western blotting assays, our findings suggested that NR2A and NR2B in the contralesional cortex were involved in EA-mediated improvements in stroke rehabilitation.

RESULTS

Electroacupuncture restored primary motor cortex forelimb motor area infarction-induced sensorimotor dysfunction

To establish a mouse unilateral ischemic stroke model with forelimb sensorimotor dysfunction, we performed photothrombotic surgery on the right primary motor cortex forelimb motor area (M1FL) (A/P: 0.74 mm, M/L: 1.5 mm) (Figures 1A and 1B).[31] Laser speckle contrast imaging (LSCI) detection showed that the blood flow in the right M1FL (infarcted area) was significantly reduced after stroke surgery, and triphenyltetrazolium chloride (TTC) staining represented the obvious ischemic foci (Figures S1A and S1B), which was not present in sham surgery animals. In the behavioral experiments testing the sensorimotor function, including the grid walking test, adhesive sticker removal test, and forelimb grip strength test, mice with stroke showed a significant increase in foot fault rate, adhesive paper touch time, adhesive paper remove time, and a decrease in grip strength (Figures S1C–S1F). Furthermore, only the ability of the left forelimb was impaired with infarction in the right M1FL (Figure S1G). These results suggest that the photothrombotic stroke mouse model induced by focal infarction with sensorimotor dysfunction was successfully established.

We next assessed whether EA stimulation could promote recovery of sensorimotor function following stroke and identified the optimal frequency for treatment. Previous clinical studies suggested that EA at 2 Hz, 50 Hz, or 100 Hz could promote functional recovery, and these three frequencies have often been selected for acupuncture treatment for other diseases, including pain, opioid addiction, insomnia, and polycystic ovary syndrome.[32–35] In this case, we validated the efficacy of the different frequencies (2 Hz, 50 Hz, and 100 Hz) of EA by performing the behavioral experiments. In the grid walking test, EA with 2 Hz was more effective than that with 100 Hz on EA 1D, 50 Hz on EA 7D, or 100 Hz on EA 7D (Figures S2A and S2B). The adhesive paper touch time and adhesive paper removal time showed similar results (Figures S2C–S2F). Together, EA with 2 Hz could improve sensorimotor-related function after stroke, including reducing the foot fault rate, adhesive paper touch time, adhesive paper removal time, and improving grip strength (Figures 1C–1M). Thus, EA stimulation with 2 Hz was used for further investigations to identify the mechanism underlying EA-mediated improvements in stroke functional recovery.
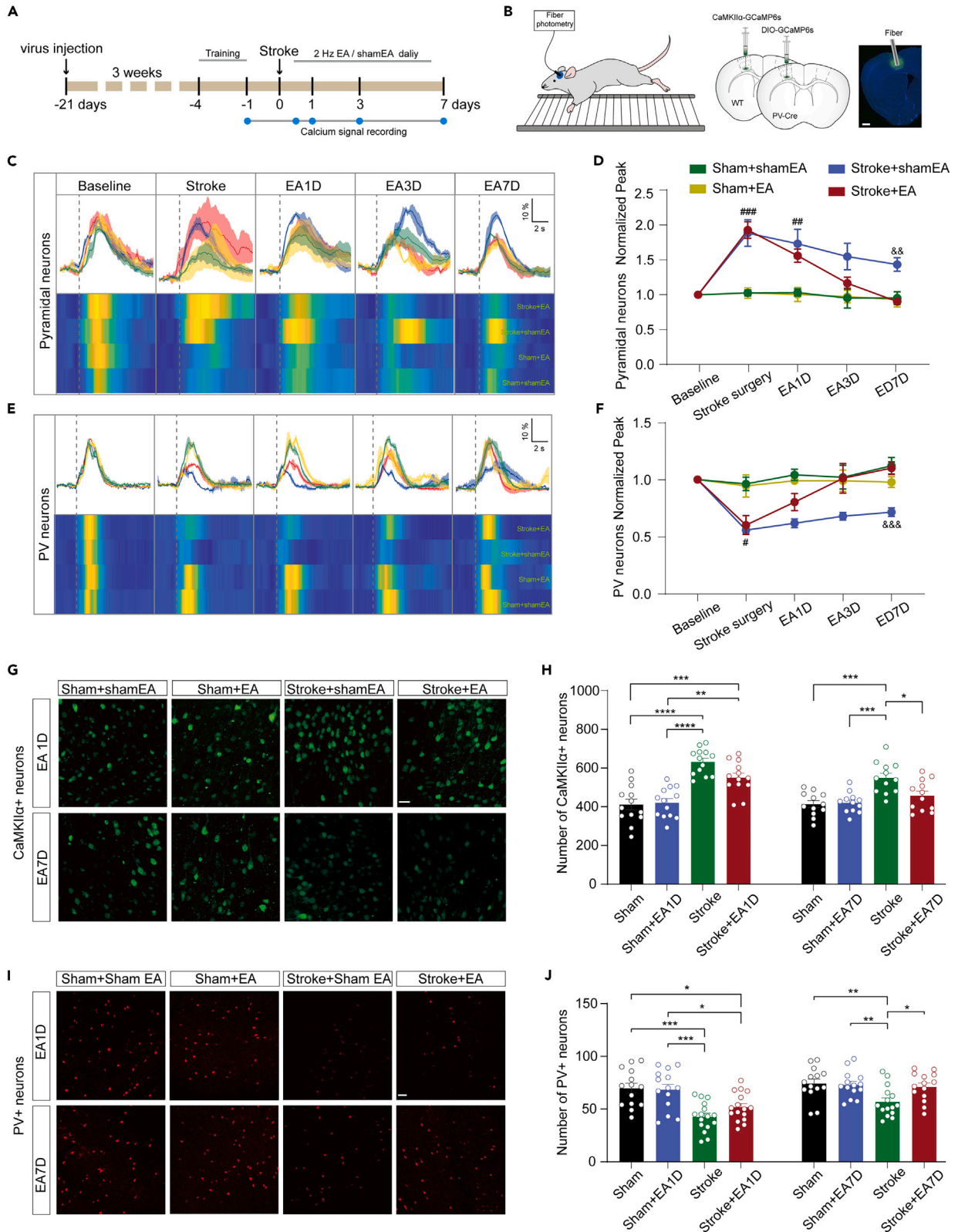
Figure 2. EA restores the stroke infarction-induced dysfunction of neuronal activity *in vivo* and expression of CAMKIIα/PV in the contralesional M1FL

(A) In mice with successful virus expression, calcium signal activity of neurons was recorded before and after stroke surgery, EA 1 day, EA 3 days, and EA 7 days, respectively.

(B) Schematic of fiber photometry of Ca2+ signals. The specific expression of GCaMP6s (green) in M1FL. Dashed lines indicated the region of inserting the optic fiber (Scale bar, 500 μm).

(C and E) Representative raw calcium signal traces (top, ΔF/F) and heatmaps illustrating the pyramidal/PV neurons Ca^{2+} signal changes (bottom). Scale bar, ΔF/F: 10%, time: 2 s.

(D) The Ca^{2+} signal of contralesional M1FL pyramidal neurons were increased in stroke mice, and EA can then rescue it. ($n = 6$ mice in Sham+EA/sham EA group; $n = 7$ mice in Stroke+EA/sham EA group).

(F) The Ca^{2+} signal of contralesional M1FL PV neurons were decreased in stroke mice, and EA can then rescue it ($n = 6$ mice in Sham+EA/sham EA group; $n = 7$ mice in Stroke+ EA group; $n = 8$ mice in Stroke+sham EA group).

(G and H) Representative images of the CAMKIIα neurons in M1FL (Scale bar, 20 μm). The expression of CAMKIIα in contralesional M1FL was increased in stroke mice, and EA can then rescue it ($n = 12$ slices per group).

(I and J) Representative images of the PV neurons in M1FL (Scale bar, 50 μm). The expression of PV in contralesional M1FL was decreased in stroke mice, and EA can then rescue it ($n = 12$ slices per group).

(D and F) Two-way analysis of variance (ANOVA) with Tukey post hoc test.

(H and J) One-way analysis of variance (ANOVA) with Tukey post hoc test, $*p < 0.05$, $**p < 0.01$, $***p < 0.001$, $****p < 0.0001$. Stroke+EA vs. Sham+EA: $^{\#}p < 0.05$; $^{\#\#}p < 0.01$, $^{\#\#\#}p < 0.001$; Stroke+EA vs. Stroke+shamEA: $^{\&\&}p < 0.01$, $^{\&\&\&}p < 0.001$. All data are represented by $mean \pm SEM$.

Electroacupuncture restored the stroke-induced disturbance of pyramidal and parvalbumin neuronal activity *in vivo* and *in vitro*

With consideration that functional recovery is tightly associated with neuronal activity,[16] we detected the neuronal activity reflecting the M1FL-mediated sensorimotor function using a fiber photometry recording technique by recording the activity of GCaMP6s-expressing pyramidal neurons or PV neurons in response to a grip stimulus at the forelimbs (Figures 2A and 2B). Specifically, we injected rAAV-CAMKIIα-GCaMP6s virus into the M1FL region in C57BL/6J mice to detect Ca^{2+} signals, representing pyramidal neuronal activity, and injected the rAAV-CAG-DIO-GCaMP6s virus into PV-Cre mice to monitor PV neuronal activity. The Ca^{2+} signaling in pyramidal neurons was obviously increased in stroke mice following the grip stimulus, and EA could alleviate this increase after the EA 3D and 7D (Figures 2C and 2D). The Ca^{2+} signal of PV neurons was significantly decreased in stroke mice, and EA could improve the attenuated PV neuronal activity (Figures 2E and 2F). Furthermore, sham EA in the stroke mice showed no effect after either 3D or 7D (Figures 2C–2F). Together, these results showed that EA could reduce pyramidal neuronal activity and increase PV neuronal activity in the contralesional M1FL after stroke.

To assess whether this disturbed neuronal activity in stroke was related to the expression level of pyramidal neurons and PV neurons, we performed immunofluorescence experiments to quantify the density of pyramidal and PV neurons with antibodies against CaMKIIα and PV after 1D or 7D following stroke surgery, respectively.[36,37] The number of pyramidal neurons was significantly increased in the stroke mice compared with that in mice with sham surgery, whereas PV neurons were conversely significantly decreased (Figures 2G–2J); this pathology could be recovered by EA stimulation. We observed no significant alteration of pyramidal and PV neurons in sham surgery mice (Figures 2G–2J). These results suggest that the expression level of pyramidal and PV neurons may contribute to the alteration of neuronal activity.

Given that the intrinsic excitability of neurons was also a factor in the modulation of neuronal activity, we detected the intrinsic excitability by *in vitro* slice patch-clamp recording in pyramidal neurons, labeled as Enhanced Green Fluorescent Protein (EGFP) using the virus with CaMKIIα as the promoter, and PV neurons, labeled as tdTomato using PV-TD transgenic mice (Figures 3A, 3B, S3A, and S3B). The results demonstrated that the parameters of the action potentials recorded from pyramidal neurons did not show any changes in either the 1D or 7D (Figures 3C–3E, S3C, and S3D). The frequency of action potentials firing and input resistance of PV neurons was attenuated after stroke; EA showed a tendency of recovery of this attenuation in the 1D and 7D (Figures 3F–3H, S3E, and S3F). In summary, enhanced pyramidal neuronal activity may be due to the increased expression of the neurons, while impaired PV neuronal activity may be attributed to both decreased expression and attenuated intrinsic excitability.

Electroacupuncture-mediated improvements were affected by the chemogenetic modulation of neuronal activity in the pyramidal and parvalbumin neurons

The above observations suggest that pyramidal and PV neuronal activity in the contralesional M1FL participates in EA-mediated stroke re-covery. Therefore, we further validated the role of pyramidal and PV neuronal activity in this process by the chemogenetic modulation (Figures 4A and 4B). Specifically, we injected the AAV-hM4Di and AAV-hM3Dq virus into the contralesional M1FL to inhibit/excite M1FL py-ramidal/PV neurons, respectively, and injected the AAV-EGFP virus as a control. We found that the inhibition of pyramidal neurons by inject-ing CaMKIIα-hM4D(Gi)-EGFP (CaMKIIα-hM4Di) can significantly improve the stroke recovery (Figures 4C and 4D). Furthermore, inhibiting PV neurons by injecting DIO-hM4D(Gi) (DIO-hM4Di) prevented rehabilitation (Figures 4E and 4F), and activating PV neurons by injecting DIO-hM3D(Gq) (DIO-hM3Dq) improved stroke recovery (Figures 4G and 4H).

Furthermore, EA plus inhibition of pyramidal neurons was more effective in the improvements of sensorimotor function than the inhibition of pyramidal neurons alone (Figures 4C and 4D), which suggests that there might be other factors participating in EA-mediated modulation besides the pyramidal neurons. Inhibition of PV neurons could partly reduce the effect of EA, and the activation of PV neurons combined with EA was shown to be more effective than the activation of PV neurons alone (Figures 4G and 4H). These results suggest that PV neuronal activity
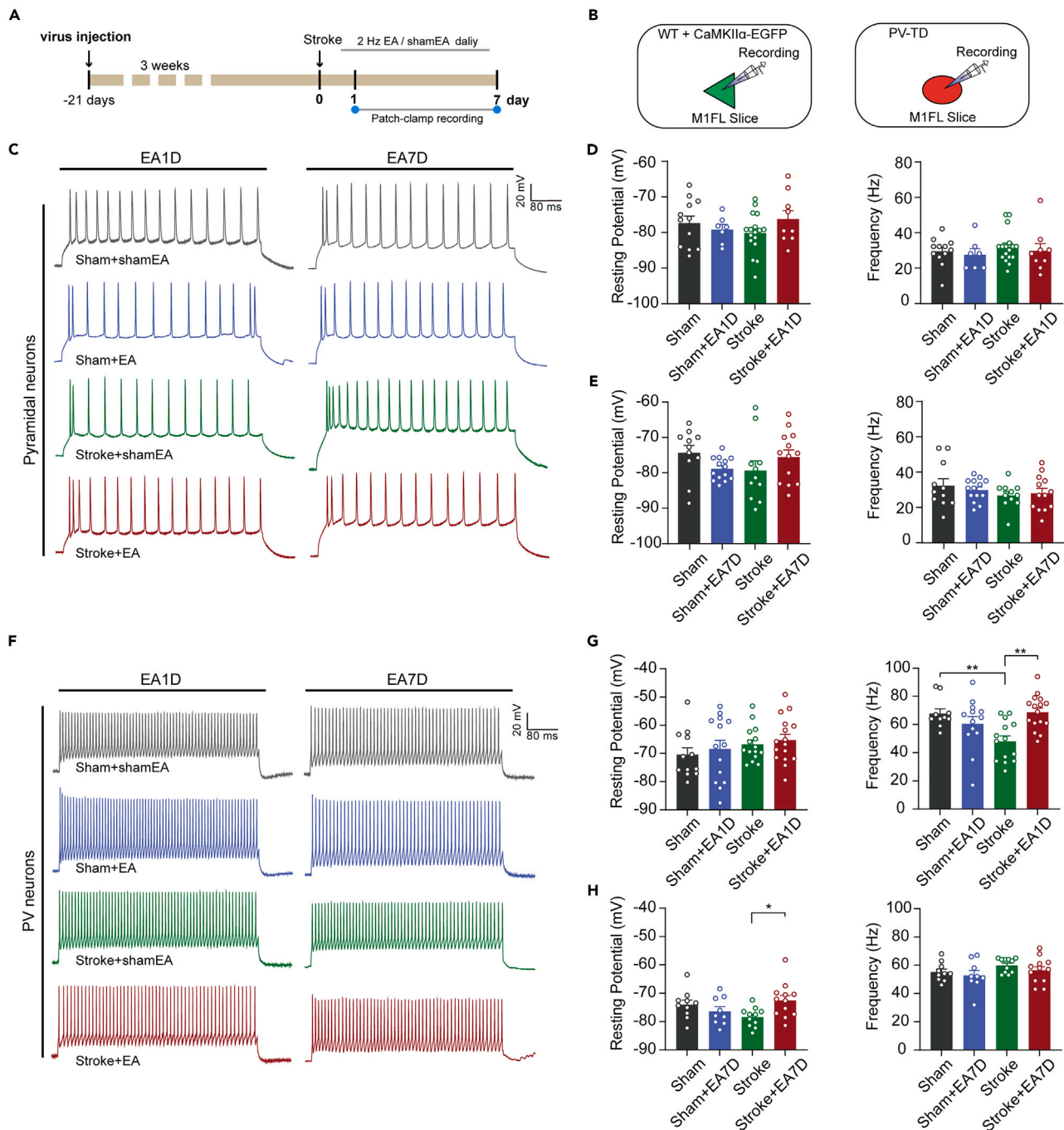
Figure 3. EA restore the stroke induced dysfunction of neuronal excitability in the contralesional M1FL *in vitro*

(A) *In vitro* electrophysiological was recorded in contralesionaM1FL mice which receiving EA or shamEA after stroke surgery 1D and 7D.

(B) Schematic of *in vitro* electrophysiological. The action electricity of pyramidal neuron and PV neuron was recorded respectively.

(C and F) Representative traces of pyramidal/PV neuron Action potential.

(D) The resting potential and spike firing frequency induced by 300 pA in pyramidal neurons were no significant difference among the groups at EA1D (Sham+shamEA, *n* = 12 cells/3 mice; Sham+EA, *n* = 7 cells/3 mice; Stroke+shamEA, *n* = 17 cells/3 mice; Stroke+EA, *n* = 9 cells/3 mice).

(E) The resting potential and spike firing frequency induced by 300 pA in pyramidal neurons were no significant difference among the groups at EA7D. (Sham+shamEA, *n* = 11 cells/3 mice; Sham+EA, *n* = 13 cells/3 mice; Stroke+shamEA, *n* = 11 cells/3 mice; Stroke+EA, *n* = 14 cells/3 mice).

(G) The spike firing frequency induced by 300 pA in PV neurons was decreased in stroke mice, and EA can then rescue it at EA1D. (Sham+shamEA, *n* = 10 cells/3 mice; Sham+EA, *n* = 13 cells/3 mice; Stroke+shamEA, *n* = 14 cells/3 mice; Stroke+EA, *n* = 16 cells/3 mice).

Figure 3. *Continued*

(H) EA could promote the resting potential induced by 300 pA in PV neurons at Stroke 7D (Sham+shamEA, *n* = 10 cells/3 mice; Sham+EA, *n* = 9 cells/3 mice; Stroke+shamEA, *n* = 11 cells/3 mice; Stroke+EA, *n* = 12 cells/3 mice).

(D, E, G and H) *One-way analysis of variance (ANOVA) with Tukey post hoc test, *p < 0.05, **p < 0.01. All data are represented by mean± SEM.*

could be also involved in the EA-mediated regulation of improvements in stroke functional recovery, in addition to the pyramidal neurons. We also observed that the injection of the control virus did not affect recovery after stroke and the efficacy of EA stimulation (Figure S4). Immunofluorescence and patch clamp validations confirmed that chemogenetics can regulate the activity of virus-labeled neurons (Figure S5). In summary, both pyramidal and PV neurons together contribute to the stroke pathology and EA-mediated improvements in stroke function.

Alteration of neuronal activity during electroacupuncture may be associated with N-methyl-D-aspartate receptor function

NMDAR is known to be a double-edge sword in stroke pathogenesis. As an excitatory glutamate receptor in the Central nervous system (CNS), it is associated with the modulation of neuronal activity; thus, we next aimed to assess the expression/function of NMDARs.[38–41] The activation of NMDARs requires glutamate binding. We first detected the glutamate level using the iGluSnFR sensor via fiber photometry recording,[42,43] which showed there was no significant alteration before and after EA in stroke surgery mice following the grip stimulus (Figures 5A and 5B). This result suggests that the glutamate level among these groups, including sham, stroke, and EA, remained comparable. Next, we investigated whether NMDAR function was altered *in vitro* using slice patch-clamp recordings. Measuring the α-amino-3-hydroxy-5-methyl-4-isoxazole-propionic acid receptor (AMPAR)/NMDAR ratio is widely used to assess the function of AMPARs or NMDARs. The result showed that a significant decrease in the AMPAR/NMDAR ratio in stroke 1D but not in stroke 7D. Interestingly, the AMPAR/NMDAR ratio in the stroke plus EA 1D group was similar to that in the control group. It is indicated that EA stimulation could, to some extent, reverse the decrease in the AMPAR/NMDAR ratio following stroke (Figures 5C and 5D). To explore the potential contribution of AMPARs to the AMPAR/NMDAR ratio, we further measured the miniature excitatory postsynaptic currents (mEPSCs), which are mostly mediated by AMPARs.[44] The increased amplitude of mEPSCs in stroke 1D suggested the enhanced function of AMPARs; thus, a decrease in the AMPAR/NMDAR ratio was mainly due to the augmentation of NMDAR-mediated responses in stroke 1D (Figures 5E and 5F). Considering that the density of NMDARs may contribute to NMDAR-mediated responses, we next assessed the levels of NR2A and NR2B in the contralesional M1FL (Figures 5G–5J). We found that the expression of NR2B increased after stroke 1D, while EA could restore its expression (Figures 5G and 5H), which could account for the enhanced NMDAR-mediated response. In contrast, the expression of NR2A in the contralesional M1FL decreased after stroke 7D, and EA could restore its expression (Figures 5I and 5J). These results suggest that disturbance of NR2A and NR2B expression could participate in the dysregulation of neuronal activity and thus in the EA-mediated improvement of stroke functional recovery.

Next, we utilized pharmacological experiments in conjunction with optical fiber recordings for validating the role of NR2A and NR2B in the neuronal activity *in vivo*. The results revealed that the both pyramidal and PV neuronal activity was significantly reduced by intraperitoneal injection the NMDAR antagonist, TCN-201 (10 mg/kg solution in DMSO, an antagonist widely used to block the NR2A-containing NMDARs) or Ro25 (10 mg/kg solution in DMSO, an antagonist widely used to block the NR2B-containing NMDARs) (Figure S6). These results suggest that both the NR2A and NR2B-containing NMDARs could regulate pyramidal and PV neuronal activity *in vivo*.

Disturbed neuronal activity in the contralesional motor cortex forelimb motor area was potentially associated with the pathology in the ipsilateral motor cortex forelimb motor area via callosum mediated-inter-inhibition

Above results demonstrated that neuronal activity in the contralesional brain regions during stroke pathogenesis was dysregulated and could be improved by EA. The mechanism of how these pathologies in the contralesional regions occurred is very likely to be an alteration in the infarcted hemisphere; bilateral brain regions tightly interact via the corpus callosum, which could mediate the interhemispheric inhibition.[45] To directly investigate the inter-inhibition from the infarcted site to the contralesional regions, we locally injected muscimol (0.9 μL of 10 mM muscimol solution in saline), an agonist of the γ-Aminobutyric acid sub-type A (GABA_A) receptor,[46] into the right M1FL (ipsilateral regions), and then implanted an electrode in the left M1FL (contralesional regions) to detect the spike firing using *in vivo* electrophysiological recordings (Figures 6A and 6B). The results showed that the pyramidal and PV neuronal activity in the left M1FL increased after enhancing the inhibition in the right M1FL (Figures 6C–6E). Next, we observed changes in the spike firing frequency of contralesional neurons after stroke surgery and EA stimulation. The results indicated that the mutual inhibition function of bilateral brain neurons is significantly reduced after stroke; EA could reverse this change (Figures 6F–6G). We then examined the expression of pyramidal and PV neurons to validate this impaired neuronal activity in the ipsilateral M1FL. Opposite to the results from the contralesional side (Figure 2), the number of pyramidal neurons in the ipsilateral M1FL was significantly decreased in the stroke mice (Figure 6H), whereas the expression of PV neurons was increased (Figure 6I). Taken together, these results indicate that EA could counteract the change in enhanced neuronal activity in the contralesional M1FL, which may be attributed to impaired inter-inhibition from the infarcted site to the contralesional regions following a stroke.

DISCUSSION

Our study results showed that EA could reduce pyramidal neuronal activity with an increase in PV neuronal activity in the contralesional M1FL, and further suggested that the NR2A and NR2B subunits of NMDARs contribute to the EA-mediated regulation of the disturbed neuronal
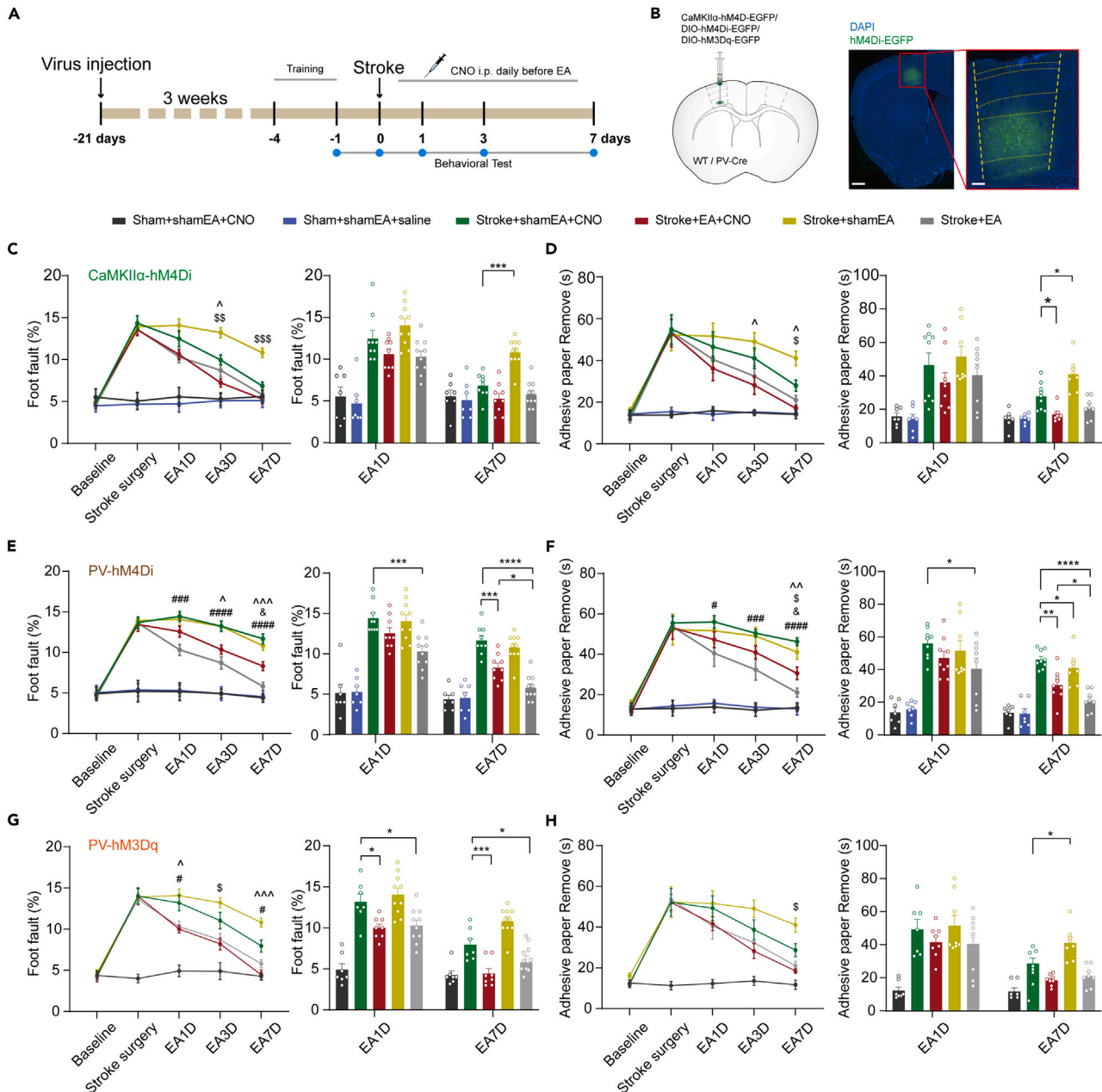
Figure 4. Both pyramidal and PV neurons contributed to the stroke pathogenesis and EA-mediated recovery

(A) Experimental procedure of chemogenetically. Chemogenetic manipulation was used in mice successfully expressing the virus, before and after stroke surgery, EA 1 day, EA 3 days, and EA 7 days to observe the EA effect and recovery after stroke (CNO: 5 mg/kg).

(B) The expression of hM4Di-EGFP (green) in M1FL (Scale bar, 500 μm).

(C and D) Chemo-inhibiting the pyramidal neurons can improve recovery in mice after stroke surgery, comparable to the effect of EA. And EA with the inhibition of pyramidal neurons was more effective to the recovery of sensorimotor function than that with the chemogenetic manipulation alone (*n* = 7 mice in Sham+shamEA+CNO/Sham+shamEA+saline, *n* = 9 mice in Stroke+shamEA+CNO/Stroke+EA+CNO, *n* = 10 mice in Stroke+shamEA/Stroke+EA).

(E and F) Chemo-inhibiting the PV neurons exacerbated the stroke-like behaviors in mice. And the inhibition of PV neurons could reduce the effect of EA to some extent (*n* = 7 mice in Sham+shamEA+CNO/Sham+shamEA+saline, *n* = 9 mice in Stroke+shamEA+CNO/Stroke+EA+CNO, *n* = 10 mice in Stroke+shamEA/Stroke+EA).

(G and H) Chemo-activating the PV neurons improved the stroke recovery, but this improvement was significantly weaker than that with EA stimulation. EA with the activation of PV neurons was more effective to the recovery of sensorimotor function than that with the chemogenetic manipulation alone (*n* = 7 mice in Sham+shamEA+CNO/Stroke+shamEA+CNO, *n* = 8 mice in Stroke+EA+CNO, *n* = 10 mice in Stroke+shamEA/Stroke+EA). (C to H) *Two-way*

Figure 4. Continued

analysis of variance (ANOVA) with *Tukey* post hoc test, *$p < 0.05$, **$p < 0.01$, ***$p < 0.001$, ****$p < 0.0001$. Stroke+EA vs. Stroke+shamEA+CNO: ####$p < 0.0001$, ###$p < 0.001$, #$p < 0.05$; Stroke+EA vs. Stroke+EA+CNO: &$p < 0.05$; Stroke+EA+CNO vs. Stroke+shamEA+CNO: ^^^$p < 0.001$, ^^$p < 0.01$, ^$p < 0.05$; Stroke+ shamEA+CNO vs. Stroke+shamEA: \$\$\$$p < 0.001$, \$\$$p < 0.01$, \$ $p < 0.05$. Recordings were performed on mice during the 9-11th week after birth. All data are represented by mean±SEM.

activity induced by stroke. These findings have deepened our understanding of the changes of excitatory and inhibitory neurons in the contralesional M1FL after stroke, and it is meaningful for exploring the mechanism by which EA promotes stroke recovery.

In recent decades, acupuncture has been demonstrated to improve functional recovery after stroke in clinical neurorehabilitation.[47] Dazhui (GV14) is acupoint commonly used for stroke treatment, which is located on the "Du meridian."[10] Although preclinical studies have shown potential mechanisms underlying acupuncture treatment in patients undergoing stroke rehabilitation, the mechanism has not been fully elucidated.[48,49] Therefore, we chose the Dazhui acupoint located on the "Du meridian" as the stimulation acupoint. Furthermore, the frequency of EA stimulation is a crucial factor in determining the efficacy of functional recovery. As has been indicated in previous studies, EA stimulation at frequencies of 2 Hz, 50 Hz, and 100 Hz has been shown to improve sensorimotor function following stroke.[31] On the other hand, these three frequencies are often selected for acupuncture stimulation, such as in the treatment of pain, opioid addiction, insomnia, and polycystic ovary syndrome.[32–35,50] However, there is a lack of further basic research to demonstrate which parameter is more effective following stroke. Through observations made in this study, we found that 2 Hz was the optimal frequency for EA stimulation to effectively improve sensorimotor-related function following stroke. These results can guide clinicians in using EA stimulation as a therapeutic in stroke rehabilitation and provide advice on stimulation frequency.

Ischemia foci causes alterations in the patterns of behavior movement activity that could extend beyond peri-infarct areas into somatotopic regions of the unaffected hemisphere as early as 30 min after stroke onset.[51,52] The contralesional hemisphere after unilateral stroke have been shown to be an important factor in functional reorganization during recovery.[14] Hence, comprehending the alterations in neuronal activity within the contralesional hemisphere during stroke and recovery is of paramount importance. Inhibitory neocortical interneurons comprise a very diverse group of cells, including those that produce cholecystokinin, somatostatin, and vasoactive intestinal peptide.[53] Among them, PV neurons are the largest class, accounting for approximately 40% of such neurons, and are important in controlling excitability in the entire brain.[19] Meanwhile, evidence has demonstrated that PV interneurons are associated with stroke pathophysiology due to their tight modulation of the excitation–inhibition balance.[24,26] Thus, PV subset inhibitory neurons was selected in this study. The role of other inhibitory neuronal types in the pathogenesis of stroke or the underlying mechanism of EA-mediated therapy requires investigation in a future study.

In the present study, *in vivo* and *in vitro* results demonstrated that the unilateral photothrombotic surgery modeling resulted in the potentiation of the pyramidal neuronal activity and attenuation of PV neuronal activity in the contralesional hemisphere. This result is consistent with previous human functional imaging studies showing increased activity of the healthy cortex after stroke.[54,55] In addition, our previously published results demonstrated a decline in the spontaneous spiking of excitatory neuronal activity in the contralesional M1; this inconsistency may be due to the methods used to detect neuronal activity.[31] Previous research utilizing multi-channel electrophysiological techniques was primarily focused on recording neuronal activity in mice under a static state. In contrast, this study employed behavioral motion coupled with optic fiber calcium imaging recording, primarily focusing on neuronal activity in functional states. Under motion states, M1FL neurons will interact with more brain regions, hence the divergence in the two research results. Of note, the results obtained by *in vitro* electrophysiological recordings suggested that the intrinsic excitability of the pyramidal neurons was not altered in the stroke or EA treatment, which was consistent with the findings of a previous study,[31] while the activity of PV neurons was attenuated after stroke. Our hypothesis is that the differential susceptibility of pyramidal and PV neurons to ischemic-like conditions is the main contributor to this phenomenon. Nahar et al. previously reported that PV interneurons are more vulnerable to the effects of oxygen glucose deprivation compared to pyramidal neurons, and the dendrites of PV interneurons exhibited more pathological beading than those of pyramidal neurons, indicating a greater degree of neuronal damage.[20] Neuronal excitability is determined by two factors, synaptic input and intrinsic excitability.[56] Our *in vivo* data demonstrated increased neuronal activity, which may be mostly attributable to synaptic input, while this input was not present *in vitro*. Bojana Kokinovic et al. also indicated that post-stroke recovery of sensory responsiveness is largely a result of changes in the synaptic inputs received by neurons in the stroke periphery rather than changes in their intrinsic excitability.[46]

Next, we investigated the mechanism underlying the change of the contralesional hemisphere related to the ipsilateral foci using *in vivo* multichannel electrophysiology and immunofluorescence. We locally injected muscimol into the infarcted site to silence the unilateral M1FL, which resulted in a significant increase in neuronal activity on the contralesional side.[46] This disinhibition from ipsilateral regions to contralesional M1FL was decreased following stroke, indicating that enhanced activation in the contralesional M1FL may be attributed to impaired inter-inhibition from the infarcted site to the contralesional regions. Subsequently, our results showed that unilateral photothrombotic surgery modeling resulted in the decreased expression of ipsilateral CaMKIIα and increased expression of PV. Zhang et al. have shown that isolated neocortex protein extracts from rats after global cerebral ischemia exhibited increased CaMKIIα immunoreactivity, which peaked at 30 min after reperfusion in the crude synaptosomal fraction.[57] On the other hand, Shohei et al. reported that CaMKIIα expression levels in the cytosolic fraction decreased by 20–40% in the penumbra and by 80% in the ischemic core area after 24 h reperfusion.[58] It is plausible that this phenomenon may be attributed to the swift recruiting of CAMKIIα at synaptic membranes subsequent to stroke, inducing neurodegeneration and fragmentation, ultimately leading to the reduced count of CaMKIIα neurons that survive 24 h after stroke. Regarding PV expression, we
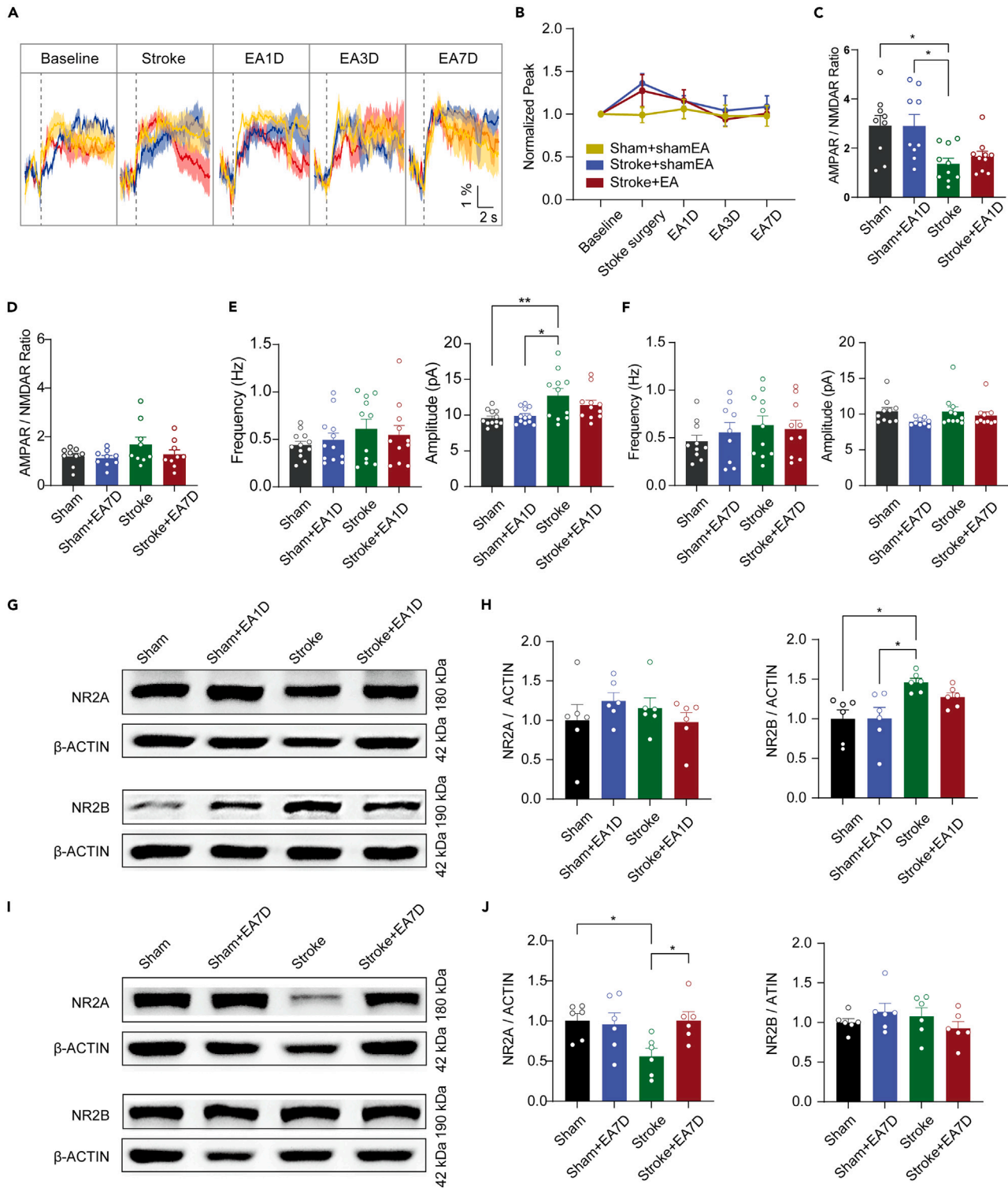
Figure 5. The alteration of neuronal activity during EA-mediated effect might be associated with the function of NMDARs

(A) Representative raw glutamate signal traces (ΔF/F). Scale bar, ΔF/F: 1%, time: 2 s.

(B) The glutamate level does not change significantly before and after EA in stroke-surgery mice following grip stimulus (*n* = 8 mice per group).

(C and D) AMPAR/NMDAR ratio was decreased at stroke 1D but not in the stroke 7D, and it does not change after EA stimulation (*n* = 9 cells from 3 Sham+shamEA/Sham+EA mice, *n* = 10 cells from 3 Stroke+shamEA/Stroke+EA mice).

Figure 5. Continued

(E and F) The amplitude of mEPSCs was increased at stroke 1D but not in the stroke 7D, and it does not happen after EA stimulation (*n* = 12 cells from 3 Sham+shamEA/Sham+EA mice, *n* = 11 cells from 3 Stroke+shamEA/Stroke+EA mice).

(G and H) Representative western blot and NR2B in the contralesional M1FL increased after stroke 1D, while acute EA could restore its expression level (*n* = 6 mice per group).

(I and J) Representative western blot and NR2A in the contralesional M1FL decreased after stroke 7D, and chronic EA could restore its expression level (*n* = 6 mice per group). (C to J) *One-way analysis of variance (ANOVA) with Tukey post hoc test.* (B) *Two-way analysis of variance (ANOVA) with Tukey post hoc test.* *$p < 0.05$, **$p < 0.01$, ***$p < 0.001$. Recordings were performed on mice during the 9-11th week after birth. All data are represented by mean ± *SEM*.

observed a marked increase in the number of PV neurons 1 day after stroke. Folweiler et al. suggested that the expression of PV neurons was increased after brain injury, which may be associated with local excitability impairments.[59]

Since the function of NMDARs is closely related to stroke and they can affect the excitability of neurons,[30] we conducted further experiments to investigate alterations in the NMDARs after stroke and EA. The results demonstrated that NR2B is upregulated in the contralesional M1FL after stroke 1D, while EA could restore its level. Consistent with these results, Barbara Picconi et al. found that both ipsilateral and contralesional hemispheres showed a significant increase in NR2B expression at 4 days after stroke.[60] The NR2B upregulation may contribute to the increased activity of pyramidal cells in the uninjured cortex. As for NR2A, it is downregulated in the contralesional M1FL after stroke 7D, while EA could restore its expression level. In contrast to these results, Liu et al. found that NR2A expression continued to increase to its peak level within 48 h after stroke, and then gradually decreased.[61] Another research study found that at 4 h after stroke, there was no significant difference in NR2A expression between the two brain hemispheres.[62] The differences observed among these results may be attributed to variations in modeling techniques and brain regions targeted in the experiments. Furthermore, the NR2A subunit plays a crucial role in synaptic plasticity; therefore, NR2A downregulation might also result in impaired NMDA receptor functions, which are required for synaptogenesis, synaptic maturation, as well as long-term plasticity. It has been suggested that the downregulation of NR2A can lower the threshold for long-term depression (LTD) and long-term potentiation (LTP), affecting the mechanism of metaplasticity.[63] The above results lead us to speculate that the enhanced expression of NR2B might be a consequence of cell death after stroke, while the downregulation of NR2A is not beneficial for stroke recovery. EA stimulation can reverse these trends, promoting recovery after stroke. In addition, NMDAR antagonists can cause severe side effects, such as nausea, vomiting, cardiovascular, and psychomimetic effects, in treated patients.[29,64] This study observed that EA can regulate NMDAR receptors after stroke, thereby possibly restoring the abnormal changes to neurons after stroke. This offers new possibilities for the acupuncture treatment of other NMDAR-related diseases.[65]

Moreover, consistent with our results, the interhemispheric imbalance model assumes that inhibition in the healthy brain is balanced between the hemispheres; however, after a stroke, there is reduced inhibition from the stroke-affected area onto the contralesional (unaffected) hemisphere.[66,67] This results in increased activity of the contralesional hemisphere, which might ultimately lead to excessive interhemispheric inhibition onto ipsilesional cortical areas.[68,69] Indeed, the restoration of symmetry in interhemispheric connections and cortical excitability after stroke does not always predict functional improvement. The recently proposed 'Bimodal Balance-Recovery' model may provide a reasonable explanation.[70] It proposes that if there is a high structural reserve, such as if some residual function remains due to the partial retention of the integrity of the neural circuitry of the corticospinal tract, then the interhemispheric imbalance model will dominate and, in these cases, it may be beneficial to utilize therapies for rebalancing interhemispheric inhibition.[71,72] For example, following an ischemic injury in M1, premotor areas can remain functional and contribute to recovery.[51,73,74] In contrast, after a large stroke, and structural reserve is low, variation will dominate, with more distant, even contralesional, areas recruited to take over lost function,[70] which may explain why severely impaired patients often retain abnormal contralesional activation.[75–77] Thus, in these cases, interhemispheric rebalancing may not be beneficial; these patients may instead benefit from the facilitation of contralesional activity.[72,78] In this study, we used unilateral photothrombotic surgery to induce unilateral focal lesions, and the brain maintained a high structural reserve. The results obtained from the chemogenetic experiments suggested that the inhibition of contralesional pyramidal neurons or activation of PV neurons (both reducing the overall of contralesional M1FL) could promote stroke recovery. Furthermore, as an economic and convenient therapeutic method, EA can relieve symptoms of ischemic stroke.[69] Our results demonstrated that the functional activity of the contralesional M1FL was significantly decreased following EA stimulation at GV14. Therefore EA stimulation could promote recovery after unilateral focal stroke by reducing the activity of pyramidal neurons and increasing the activity of PV neurons in the contralesional M1FL, similar to previous clinical studies on the theta-burst stimulation of the contralesional M1 for the promotion of upper limb recovery after stroke.[79] The results suggest that EA may affect stroke rehabilitation by modulating the activity of neurons in the contralesional and ipsilateral cortex as well as the corpus callosum.

In summary, the results of the present study suggest that EA stimulation could potentially ameliorate the disrupted neuronal activity caused by stroke pathogenesis, and that NMDARs contributed to this process, ultimately leading to improved sensorimotor ability after a stroke. Additionally, the study highlights the crucial role of the contralesional cortex in the recovery process following unilateral stroke.

Limitations of the study

Firstly, we do not explore the involvement of other types of inhibitory interneurons, such as those that release cholecystokinin, somatostatin, and vasoactive intestinal peptide, in the effects of EA after stroke. Secondly, pyramidal neuronal activity after the chemo-manipulation of PV neurons, or PV neuronal activity after the chemo-manipulation of pyramidal neurons, could be indirectly affected. However, it is hard to distinguish this indirect influence of another neuronal type for the complex systems by *in vivo* exogenous manipulation. Thirdly, the effect of NMDARs to the long-term plasticity carries substantial research importance and benefits the interpretability of the results; while it was not
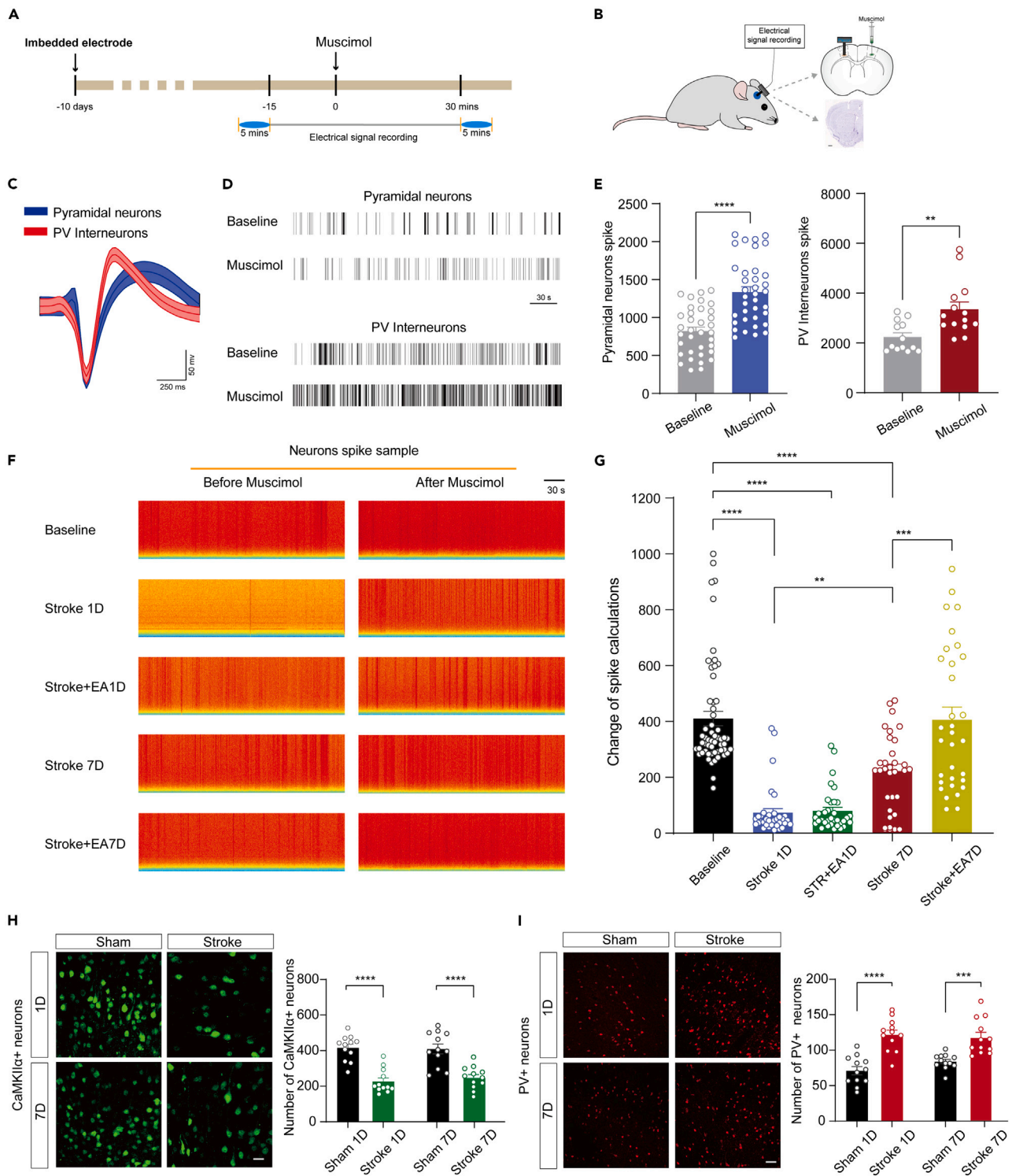
Figure 6. Contralesional and ipsilateral M1FL Pyramidal/PV neurons were reciprocally regulated via callosum mediated-interinhibition

(A) Experimental procedure of muscimol administration *in vivo* multichannel electrophysiology. Ten days after multi-channel electrodes were implanted in the right M1FL, neuron spike was recorded within 5 min before and after muscimol (0.9 μL of 10 mM solution in saline, GABA$_A$ receptor antagonists) administration in left M1FL.

(B) Schematic of *in vivo* multichannel electrophysiology. Nissner staining confirms the placement of electrodes (Scale bar, 1 mm).

Figure 6. Continued

(C) Waveform analysis revealed distinct cell type units. PV neurons with short spike width and pyramidal neurons with long spike width. Scale bar, 50 mV, time: 250 ms.

(D) Representative raster plot showing that a clear increase in neuron spike after muscimol administration (Scale bar, 30 s).

(E) A clear increase in pyramidal neurons and PV neurons spike after muscimol administration (n = 5 mice per group).

(F) Representative spectrogram showing a decrease in neuronal spike after stoke and an increase after muscimol administration (Scale bar, 30 s).

(G) The increasing of pyramidal neurons and PV neurons spike after muscimol administration decreases after stroke (n = 5 mice per group).

(H and I) Representative images of the CAMKIIα neurons in ipsilateral M1FL (Scale bar, 20 μm). The expression of CaMKIIα in ipsilateral M1FL was decreased in stroke mice (n = 12 slices per group).

(C and D) Representative images of the PV neurons in ipsilateral M1FL (Scale bar, 50 μm). The expression of PV in ipsilateral M1FL was increased in stroke mice (n = 12 slices per group).

(E, H, and I) Student's t test, ** p < 0.01, *** p < 0.001, **** p < 0.0001. Recordings were performed on mice during the 9-11th week after birth. All data are represented by $mean \pm SEM$.

included in the research conducted for this article. Fourthly, the phototrombosis-induced stroke model we adopted highly simulates the changes in local cerebral cortical infarction while the infarct region is often potentially larger in the clinical practice. Future research should consider these issues and further investigate the potential impact of EA after stroke.

STAR★METHODS

Detailed methods are provided in the online version of this paper and include the following:

- KEY RESOURCES TABLE
- RESOURCE AVAILABILITY
  - Lead contact
  - Materials availability
  - Data and code availability
- EXPERIMENTAL MODEL AND STUDY PARTICIPANT DETAILS
  - Animals and housing conditions
- METHOD DETAILS
  - Photothrombotic model surgery procedures
  - Behavioral tests
  - Virus injection
  - Fiber photometry
  - *In vivo* pharmacogenetic manipulations
  - *In vivo* multichannel electrophysiology
  - *In vitro* electrophysiological recording
  - EA stimulation treatment
  - Histological assessment
  - Western Blot
- QUANTIFICATION AND STATISTICAL ANALYSIS

SUPPLEMENTAL INFORMATION

Supplemental information can be found online at https://doi.org/10.1016/j.isci.2024.109695.

AUTHOR CONTRIBUTIONS

Lulu Yao, Nenggui Xu, and Xiaorong Tang designed all experiments. Xiaorong Tang, Jiahui Shi, Shumin Lin, Zhiyin He, Wenhui Di, Siyun Chen, Xiaoyun Yang, Ying Shang, and Zhaoxiang Zhang performed the experiments. Xiaorong Tang, Jiahui Shi, Junshang Wu, Qiuping Ye, and Liming Lu analyzed the data. Chunzhi Tang, Lin Wang, Shuai Cui, and Yuan Si contributed to discussion. Lulu Yao, Nenggui Xu, Xiaorong Tang,

REFERENCES

1. Feigin, V.L., Brainin, M., Norrving, B., Martins, S., Sacco, R.L., Hacke, W., Fisher, M., Pandian, J., and Lindsay, P. (2022). World Stroke Organization (WSO): Global Stroke Fact Sheet 2022. Int. J. Stroke 17, 18–29. https://doi.org/10.1177/17474930211065917.

2. Owolabi, M.O., Thrift, A.G., Mahal, A., Ishida, M., Martins, S., Johnson, W.D., Pandian, J., Abd-Allah, F., Yaria, J., Phan, H.T., et al. (2022). Primary stroke prevention worldwide: translating evidence into action. Lancet Public Health 7, e74–e85. https://doi.org/10.1016/S2468-2667(21)00230-9.

3. Jackson, G., and Chari, K. (2019). National Hospital Care Survey Demonstration Projects: Stroke Inpatient Hospitalizations. Natl. Health Stat. Report. 1–11.

4. Yaghi, S., Bernstein, R.A., Passman, R., Okin, P.M., and Furie, K.L. (2017). Cryptogenic Stroke: Research and Practice. Circ. Res. 120, 527–540. https://doi.org/10.1161/CIRCRESAHA.116.308447.

5. Hollist, M., Morgan, L., Cabatbat, R., Au, K., Kirmani, M.F., and Kirmani, B.F. (2021). Acute Stroke Management: Overview and Recent Updates. Aging Dis. 12, 1000–1009. https://doi.org/10.14336/AD.2021.0311.

6. Anaya, M.A., and Branscheidt, M. (2019). Neurorehabilitation After Stroke. Stroke 50, e180–e182. https://doi.org/10.1161/STROKEAHA.118.023878.

7. Maier, M., Ballester, B.R., and Verschure, P.F.M.J. (2019). Principles of Neurorehabilitation After Stroke Based on Motor Learning and Brain Plasticity Mechanisms. Front. Syst. Neurosci. 13, 74. https://doi.org/10.3389/fnsys.2019.00074.

8. Jun, M.H., Kim, Y.M., and Kim, J.U. (2015). Modern acupuncture-like stimulation methods: a literature review. Integr. Med. Res. 4, 195–219. https://doi.org/10.1016/j.imr.2015.09.005.

9. Liu, A.J., Li, J.H., Li, H.Q., Fu, D.L., Lu, L., Bian, Z.X., and Zheng, G.Q. (2015). Electroacupuncture for Acute Ischemic Stroke: A Meta-Analysis of Randomized Controlled Trials. Am. J. Chin. Med. 43, 1541–1566. https://doi.org/10.1142/S0192415X15500883.

10. Chang, Q.Y., Lin, Y.W., and Hsieh, C.L. (2018). Acupuncture and neuroregeneration in ischemic stroke. Neural Regen. Res. 13, 573–583. https://doi.org/10.4103/1673-5374.230272.

11. Feng, R., and Zhang, F. (2014). The neuroprotective effect of electro-acupuncture against ischemic stroke in animal model: a review. Afr. J. Tradit., Complementary Altern. Med. 11, 25–29. https://doi.org/10.4314/ajtcam.v11i3.5.

12. Xing, Y., Zhang, M., Li, W.B., Dong, F., and Zhang, F. (2018). Mechanisms Involved in the Neuroprotection of Electroacupuncture Therapy for Ischemic Stroke. Front. Neurosci. 12, 929. https://doi.org/10.3389/fnins.2018.00929.

13. Crofts, A., Kelly, M.E., and Gibson, C.L. (2020). Imaging Functional Recovery Following Ischemic Stroke: Clinical and Preclinical fMRI Studies. J. Neuroimaging 30, 5–14. https://doi.org/10.1111/jon.12668.

14. Buetefisch, C.M. (2015). Role of the Contralesional Hemisphere in Post-Stroke Recovery of Upper Extremity Motor Function. Front. Neurol. 6, 214. https://doi.org/10.3389/fneur.2015.00214.

15. Liu, W., He, X., Lin, H., Yang, M., Dai, Y., Chen, L., Li, C., Liang, S., Tao, J., and Chen, L. (2023). Ischemic stroke rehabilitation through optogenetic modulation of parvalbumin neurons in the contralateral motor cortex. Exp. Neurol. 360, 114289. https://doi.org/10.1016/j.expneurol.2022.114289.

16. Xie, Y., Chen, S., Wu, Y., and Murphy, T.H. (2014). Prolonged deficits in parvalbumin neuron stimulation-evoked network activity despite recovery of dendritic structure and excitability in the somatosensory cortex following global ischemia in mice. J. Neurosci. 34, 14890–14900. https://doi.org/10.1523/jneurosci.1775-14.2014.

17. Kwon, Y.H., and Lee, M.Y. (2014). Changes in cortical activation patterns accompanying somatosensory recovery in a stroke patient: a functional magnetic resonance imaging study. Neural Regen. Res. 9, 1485–1488. https://doi.org/10.4103/1673-5374.139468.

18. Espuny-Camacho, I., Michelsen, K.A., Gall, D., Linaro, D., Hasche, A., Bonnefont, J., Bali, C., Orduz, D., Bilheu, A., Herpoel, A., et al. (2013). Pyramidal neurons derived from human pluripotent stem cells integrate efficiently into mouse brain circuits in vivo. Neuron 77, 440–456. https://doi.org/10.1016/j.neuron.2012.12.011.

19. Druga, R., Salaj, M., and Al-Redouan, A. (2023). Parvalbumin - Positive Neurons in the Neocortex: A Review. Physiol. Res. 72. S173-s191. https://doi.org/10.33549/physiolres.935005.

20. Nahar, L., Delacroix, B.M., and Nam, H.W. (2021). The Role of Parvalbumin Interneurons in Neurotransmitter Balance and Neurological Disease. Front. Psychiatr. 12, 679960. https://doi.org/10.3389/fpsyt.2021.679960.

21. Petilla Interneuron Nomenclature Group, Ascoli, G.A., Alonso-Nanclares, L., Anderson, S.A., Barrionuevo, G., Benavides-Piccione, R., Burkhalter, A., Buzsáki, G., Cauli, B., Defelipe, J., et al. (2008). Petilla terminology: nomenclature of features of GABAergic interneurons of the cerebral cortex. Nat. Rev. Neurosci. 9, 557–568. https://doi.org/10.1038/nrn2402.

22. Wilson, N.R., Runyan, C.A., Wang, F.L., and Sur, M. (2012). Division and subtraction by distinct cortical inhibitory networks in vivo. Nature 488, 343–348. https://doi.org/10.1038/nature11347.

23. Foster, V., Oakley, A.E., Slade, J.Y., Hall, R., Polvikoski, T.M., Burke, M., Thomas, A.J., Khundakar, A., Allan, L.M., and Kalaria, R.N. (2014). Pyramidal neurons of the prefrontal cortex in post-stroke, vascular and other ageing-related dementias. Brain 137, 2509–2521. https://doi.org/10.1093/brain/awu172.

24. Povysheva, N., Nigam, A., Brisbin, A.K., Johnson, J.W., and Barrionuevo, G. (2019). Oxygen-Glucose Deprivation Differentially Affects Neocortical Pyramidal Neurons and Parvalbumin-Positive Interneurons. Neuroscience 412, 72–82. https://doi.org/10.1016/j.neuroscience.2019.05.042.

25. Spruston, N. (2008). Pyramidal neurons: dendritic structure and synaptic integration. Nat. Rev. Neurosci. 9, 206–221. https://doi.org/10.1038/nrn2286.

26. Brown, J.A., Ramikie, T.S., Schmidt, M.J., Báldi, R., Garbett, K., Everheart, M.G., Warren, L.E., Gellért, L., Horváth, S., Patel, S., and Mirnics, K. (2015). Inhibition of parvalbumin-expressing interneurons results in complex behavioral changes. Mol. Psychiatr. 20, 1499–1507. https://doi.org/10.1038/mp.2014.192.

27. Jewett, B.E., and Thapa, B. (2022). Physiology, NMDA Receptor.

28. Zhou, X., Chen, Z., Yun, W., and Wang, H. (2015). NMDA receptor activity determines neuronal fate: location or number? Rev. Neurosci. 26, 39–47. https://doi.org/10.1515/revneuro-2014-0053.

29. Wu, Q.J., and Tymianski, M. (2018). Targeting NMDA receptors in stroke: new hope in neuroprotection. Mol. Brain 11, 15. https://doi.org/10.1186/s13041-018-0357-8.

30. Ge, Y., Chen, W., Axerio-Cilies, P., and Wang, Y.T. (2020). NMDARs in Cell Survival and Death: Implications in Stroke Pathogenesis and Treatment. Trends Mol. Med. 26, 533–551. https://doi.org/10.1016/j.molmed.2020.03.001.

31. Yao, L.-L., Yuan, S., Wu, Z.-N., Luo, J.-Y., Tang, X.-R., Tang, C.-Z., Cui, S., and Xu, N.-G. (2022). Contralateral S1 function is involved in electroacupuncture treatment-mediated recovery after focal unilateral M1 infarction. Neural Regen. Res. 17, 1310–1317. https://doi.org/10.4103/1673-5374.327355.

32. Jedel, E., Labrie, F., Odén, A., Holm, G., Nilsson, L., Janson, P.O., Lind, A.K., Ohlsson, C., and Stener-Victorin, E. (2011). Impact of electro-acupuncture and physical exercise on hyperandrogenism and oligo/amenorrhea in women with polycystic ovary syndrome: a randomized controlled trial. Am. J. Physiol. Endocrinol. Metab. 300, E37–E45. https://doi.org/10.1152/ajpendo.00495.2010.

33. Liu, C., Zheng, S., Wu, W., Wang, X., Qin, S., Zhao, Y., Xi, H., and Wan, Q. (2019). Effects of acupuncture on the hypothalamus-pituitary-adrenal axis in chronic insomnia patients: a study protocol for a randomized controlled trial. Trials 20, 810. https://doi.org/10.1186/s13063-019-3964-5.

34. Sha, L., Weiqian, T., JI, Z.F., YAO, S., Fengzhen, Yang, T., and Minghui, Z. (2023). Clinical observation of electroacupuncture relieving opioid resistance in cancer pain patients. Shanghai J. Acupunct. Moxibustion 42, 889–894. https://doi.org/10.13460/j.issn.1005-0957.2023.09.0889.

35. Huang, C., Wang, Y., Chang, J.K., and Han, J.S. (2000). Endomorphin and mu-opioid receptors in mouse brain mediate the analgesic effect produced by 2 Hz but not 100 Hz electroacupuncture stimulation. Neurosci. Lett. 294, 159–162. https://doi.org/10.1016/s0304-3940(00)01572-x.

36. Zalcman, G., Federman, N., and Romano, A. (2018). CaMKII Isoforms in Learning and Memory: Localization and Function. Front. Mol. Neurosci. 11, 445. https://doi.org/10.3389/fnmol.2018.00445.

37. Hu, H., Gan, J., and Jonas, P. (2014). Interneurons. Fast-spiking, parvalbumin⁺ GABAergic interneurons: from cellular design to microcircuit function. Science 345, 1255263. https://doi.org/10.1126/science.1255263.

38. Holmes, A.R., Castellino, F.J., and Balsara, R.D. (2018). The Dichotomous Role of N-methyl- D- Aspartate Receptors in Ischemic Stroke. J. Cardiol. Cardiovasc. Sci. 2. https://doi.org/10.29245/2578-3025/2018/4.113.

39. Xue, J.-G., Masuoka, T., Gong, X.-D., Chen, K.-S., Yanagawa, Y., Law, S.K.A., and Konishi, S. (2011). NMDA receptor activation enhances inhibitory GABAergic transmission onto hippocampal pyramidal neurons via presynaptic and postsynaptic mechanisms. J. Neurophysiol. 105, 2897–2906. https://doi.org/10.1152/jn.00287.2010.

40. Wu, L.J., Toyoda, H., Zhao, M.G., Lee, Y.S., Tang, J., Ko, S.W., Jia, Y.H., Shum, F.W.F., Zerbinatti, C.V., Bu, G., et al. (2005). Upregulation of Forebrain NMDA NR2B Receptors Contributes to Behavioral Sensitization after Inflammation. J. Neurosci. 25, 11107–11116. https://doi.org/10.1523/JNEUROSCI.1678-05.2005.

41. Varga, E., Juhász, G., Bozsó, Z., Penke, B., Fülöp, L., and Szegedi, V. (2014). Abeta(1-42) Enhances Neuronal Excitability in the CA1 via NR2B Subunit-Containing NMDA Receptors. Neural Plast. 2014, 584314. https://doi.org/10.1155/2014/584314.

42. Marvin, J.S., Scholl, B., Wilson, D.E., Podgorski, K., Kazemipour, A., Müller, J.A., Schoch, S., Quiroz, F.J.U., Rebola, N., Bao, H., et al. (2018). Stability, affinity, and chromatic variants of the glutamate sensor iGluSnFR. Nat. Methods 15, 936–939. https://doi.org/10.1038/s41592-018-0171-3.

43. Marvin, J.S., Borghuis, B.G., Tian, L., Cichon, J., Harnett, M.T., Akerboom, J., Gordus, A., Renninger, S.L., Chen, T.W., Bargmann, C.I., et al. (2013). An optimized fluorescent probe for visualizing glutamate neurotransmission. Nat. Methods 10, 162–170. https://doi.org/10.1038/nmeth.2333.

44. Chater, T.E., and Goda, Y. (2022). The Shaping of AMPA Receptor Surface Distribution by Neuronal Activity. Front. Synaptic Neurosci. 14, 833782. https://doi.org/10.3389/fnsyn.2022.833782.

45. Palmer, L.M., Schulz, J.M., Murphy, S.C., Ledergerber, D., Murayama, M., and Larkum, M.E. (2012). The Cellular Basis of GABAB-Mediated Interhemispheric Inhibition. Science 335, 989–993. https://doi.org/10.1126/science.1217276.

46. Kokinovic, B., and Medini, P. (2018). Loss of GABA(B) -mediated interhemispheric synaptic inhibition in stroke periphery. J. Physiol. 596, 1949–1964. https://doi.org/10.1113/JP275690.

47. Wu, P., Mills, E., Moher, D., and Seely, D. (2010). Acupuncture in poststroke rehabilitation: a systematic review and meta-analysis of randomized trials. Stroke 41, e171–e179. https://doi.org/10.1161/strokeaha.109.573576.

48. Wang, W.W., Xie, C.L., Lu, L., and Zheng, G.Q. (2014). A systematic review and meta-analysis of Baihui (GV20)-based scalp acupuncture in experimental ischemic stroke. Sci. Rep. 4, 3981. https://doi.org/10.1038/srep03981.

49. Lu, L., Zhang, X.G., Zhong, L.L.D., Chen, Z.X., Li, Y., Zheng, G.Q., and Bian, Z.X. (2016). Acupuncture for neurogenesis in experimental ischemic stroke: a systematic review and meta-analysis. Sci. Rep. 6, 19521. https://doi.org/10.1038/srep19521.

50. Ogata, A., Sugenoya, J., Nishimura, N., and Matsumoto, T. (2005). Low and high frequency acupuncture stimulation inhibits mental stress-induced sweating in humans via different mechanisms. Auton. Neurosci. 118, 93–101. https://doi.org/10.1016/j.autneu.2004.11.008.

51. Murphy, T.H., and Corbett, D. (2009). Plasticity during stroke recovery: from synapse to behaviour. Nat. Rev. Neurosci. 10, 861–872. https://doi.org/10.1038/nrn2735.

52. Mohajerani, M.H., Aminoltejari, K., and Murphy, T.H. (2011). Targeted mini-strokes produce changes in interhemispheric sensory signal processing that are indicative of disinhibition within minutes. Proc. Natl. Acad. Sci. USA 108, E183–E191. https://doi.org/10.1073/pnas.1101914108.

53. Kepecs, A., and Fishell, G. (2014). Interneuron cell types are fit to function. Nature 505, 318–326. https://doi.org/10.1038/nature12983.

54. Marshall, R.S., Perera, G.M., Lazar, R.M., Krakauer, J.W., Constantine, R.C., and DeLaPaz, R.L. (2000). Evolution of cortical activation during recovery from corticospinal tract infarction. Stroke 31, 656–661. https://doi.org/10.1161/01.str.31.3.656.

55. Ward, N.S., and Cohen, L.G. (2004). Mechanisms underlying recovery of motor function after stroke. Arch. Neurol. 61, 1844–1848. https://doi.org/10.1001/archneur.61.12.1844.

56. van Vreeswijk, C., and Sompolinsky, H. (1996). Chaos in neuronal networks with balanced excitatory and inhibitory activity. Science 274, 1724–1726. https://doi.org/10.1126/science.274.5293.1724.

57. Zhang, X., Connelly, J., Levitan, E.S., Sun, D., and Wang, J.Q. (2021). Calcium/Calmodulin-Dependent Protein Kinase II in Cerebrovascular Diseases. Transl. Stroke Res. 12, 513–529. https://doi.org/10.1007/s12975-021-00901-9.

58. Matsumoto, S., Shamloo, M., Matsumoto, E., Isshiki, A., and Wieloch, T. (2004). Protein kinase C-gamma and calcium/calmodulin-dependent protein kinase II-alpha are persistently translocated to cell membranes of the rat brain during and after middle cerebral artery occlusion. J. Cerebr. Blood Flow Metab. 24, 54–61. https://doi.org/10.1097/01.WCB.0000095920.70924.F5.

59. Folweiler, K.A., Xiong, G., Best, K.M., Metheny, H.E., Nah, G., and Cohen, A.S. (2020). Traumatic Brain Injury Diminishes Feedforward Activation of Parvalbumin-Expressing Interneurons in the Dentate Gyrus. eNeuro 7. https://doi.org/10.1523/ENEURO.0195-19.2020.

60. Picconi, B., Tortiglione, A., Barone, I., Centonze, D., Gardoni, F., Gubellini, P., Bonsi, P., Pisani, A., Bernardi, G., Di Luca, M., and Calabresi, P. (2006). NR2B subunit exerts a critical role in postischemic synaptic plasticity. Stroke 37, 1895–1901. https://doi.org/10.1161/01.STR.0000226981.57777.b0.

61. Liu, Z., Zhao, W., Xu, T., Pei, D., and Peng, Y. (2010). Alterations of NMDA receptor subunits NR1, NR2A and NR2B mRNA expression and their relationship to apoptosis following transient forebrain ischemia. Brain Res. 1361, 133–139. https://doi.org/10.1016/j.brainres.2010.09.035.

62. Cui, Z., Feng, R., Jacobs, S., Duan, Y., Wang, H., Cao, X., and Tsien, J.Z. (2013). Increased NR2A:NR2B ratio compresses long-term depression range and constrains long-term memory. Sci. Rep. 3, 1036. https://doi.org/10.1038/srep01036.

63. Massey, P.V., Johnson, B.E., Moult, P.R., Auberson, Y.P., Brown, M.W., Molnar, E., Collingridge, G.L., and Bashir, Z.I. (2004). Differential roles of NR2A and NR2B-containing NMDA receptors in cortical long-term potentiation and long-term depression. J. Neurosci. 24, 7821–7828. https://doi.org/10.1523/jneurosci.1697-04.2004.

64. Diener, H.C., AlKhedr, A., Busse, O., Hacke, W., Zingmark, P.H., Jonsson, N., and Basun, H.; Study group (2002). Treatment of acute ischaemic stroke with the low-affinity, use-dependent NMDA antagonist AR-R15896AR. A safety and tolerability study. J. Neurol. 249, 561–568. https://doi.org/10.1007/s004150200065.

65. Yu, B.H., Xing, Y., and Zhang, F. (2020). The Therapeutic Effect of Electroacupuncture Therapy for Ischemic Stroke. Evid. Based. Complement. Alternat. Med. 2020, 6415083. https://doi.org/10.1155/2020/6415083.

66. Pavlova, E.L., Semenov, R.V., Pavlova-Deb, M.P., and Guekht, A.B. (2022). Transcranial direct current stimulation of the premotor cortex aimed to improve hand motor function in chronic stroke patients. Brain Res. 1780, 147790. https://doi.org/10.1016/j.brainres.2022.147790.

67. Murase, N., Duque, J., Mazzocchio, R., and Cohen, L.G. (2004). Influence of interhemispheric interactions on motor function in chronic stroke. Ann. Neurol. 55, 400–409. https://doi.org/10.1002/ana.10848.

68. Kirton, A., Deveber, G., Gunraj, C., and Chen, R. (2010). Cortical excitability and interhemispheric inhibition after subcortical pediatric stroke: plastic organization and effects of rTMS. Clin. Neurophysiol. *121*, 1922–1929. https://doi.org/10.1016/j.clinph.2010.04.021.

69. Liepert, J., Hamzei, F., and Weiller, C. (2000). Motor cortex disinhibition of the unaffected hemisphere after acute stroke. Muscle Nerve *23*, 1761–1763. https://doi.org/10.1002/1097-4598(200011)23:11<1761::aid-mus14>3.0.co;2-m.

70. Di Pino, G., Pellegrino, G., Assenza, G., Capone, F., Ferreri, F., Formica, D., Ranieri, F., Tombini, M., Ziemann, U., Rothwell, J.C., and Di Lazzaro, V. (2014). Modulation of brain plasticity in stroke: a novel model for neurorehabilitation. Nat. Rev. Neurol. *10*, 597–608. https://doi.org/10.1038/nrneurol.2014.162.

71. Wessel, M.J., Egger, P., and Hummel, F.C. (2021). Predictive models for response to non-invasive brain stimulation in stroke: A critical review of opportunities and pitfalls. Brain Stimul. *14*, 1456–1466. https://doi.org/10.1016/j.brs.2021.09.006.

72. Plow, E.B., Sankarasubramanian, V., Cunningham, D.A., Potter-Baker, K., Varnerin, N., Cohen, L.G., Sterr, A., Conforto, A.B., and Machado, A.G. (2016). Models to Tailor Brain Stimulation Therapies in Stroke. Neural Plast. *2016*, 4071620. https://doi.org/10.1155/2016/4071620.

73. Alia, C., Spalletti, C., Lai, S., Panarese, A., Lamola, G., Bertolucci, F., Vallone, F., Di Garbo, A., Chisari, C., Micera, S., and Caleo, M. (2017). Neuroplastic Changes Following Brain Ischemia and their Contribution to Stroke Recovery: Novel Approaches in Neurorehabilitation. Front. Cell. Neurosci. *11*, 76. https://doi.org/10.3389/fncel.2017.00076.

74. Dancause, N., and Nudo, R.J. (2011). Shaping plasticity to enhance recovery after injury. Prog. Brain Res. *192*, 273–295. https://doi.org/10.1016/B978-0-444-53355-5.00015-4.

75. Bradnam, L.V., Stinear, C.M., Barber, P.A., and Byblow, W.D. (2012). Contralesional hemisphere control of the proximal paretic upper limb following stroke. Cerebr. Cortex *22*, 2662–2671. https://doi.org/10.1093/cercor/bhr344.

76. Bestmann, S., Swayne, O., Blankenburg, F., Ruff, C.C., Teo, J., Weiskopf, N., Driver, J., Rothwell, J.C., and Ward, N.S. (2010). The role of contralesional dorsal premotor cortex after stroke as studied with concurrent TMS-fMRI. J. Neurosci. *30*, 11926–11937. https://doi.org/10.1523/JNEUROSCI.5642-09.2010.

77. Schlaug, G., Renga, V., and Nair, D. (2008). Transcranial direct current stimulation in stroke recovery. Arch. Neurol. *65*, 1571–1576. https://doi.org/10.1001/archneur.65.12.1571.

78. Qin, L., Actor-Engel, H.S., Woo, M.S., Shakil, F., Chen, Y.W., Cho, S., and Aoki, C. (2019). An Increase of Excitatory-to-Inhibitory Synaptic Balance in the Contralateral Cortico-Striatal Pathway Underlies Improved Stroke Recovery in BDNF Val66Met SNP Mice. Neurorehabilitation Neural Repair *33*, 989–1002. https://doi.org/10.1177/1545968319872997.

79. Vink, J.J.T., van Lieshout, E.C.C., Otte, W.M., van Eijk, R.P.A., Kouwenhoven, M., Neggers, S.F.W., van der Worp, H.B., Visser-Meily, J.M.A., and Dijkhuizen, R.M. (2023). Continuous Theta-Burst Stimulation of the Contralesional Primary Motor Cortex for Promotion of Upper Limb Recovery After Stroke: A Randomized Controlled Trial. Stroke *54*, 1962–1971. https://doi.org/10.1161/strokeaha.123.042924.

80. Cui, S., Yao, S., Wu, C., Yao, L., Huang, P., Chen, Y., Tang, C., and Xu, N. (2020). Electroacupuncture Involved in Motor Cortex and Hypoglossal Neural Control to Improve Voluntary Swallowing of Poststroke Dysphagia Mice. Neural Plast. *2020*, 8857543. https://doi.org/10.1155/2020/8857543.

81. Wu, C., Zhao, L., Li, X., Xu, Y., Guo, H., Huang, Z., Wang, Q., Liu, H., Chen, D., and Zhu, M. (2021). Integrated Bioinformatics Analysis of Potential mRNA and miRNA Regulatory Networks in Mice With Ischemic Stroke Treated by Electroacupuncture. Front. Neurol. *12*, 719354. https://doi.org/10.3389/fneur.2021.719354.

82. Li, Y., Liu, Z., Guo, Q., and Luo, M. (2019). Long-term Fiber Photometry for Neuroscience Studies. Neurosci. Bull. *35*, 425–433. https://doi.org/10.1007/s12264-019-00379-4.

83. Terashima, A., Cotton, L., Dev, K.K., Meyer, G., Zaman, S., Duprat, F., Henley, J.M., Collingridge, G.L., and Isaac, J.T.R. (2004). Regulation of synaptic strength and AMPA receptor subunit composition by PICK1. J. Neurosci. *24*, 5381–5390. https://doi.org/10.1523/jneurosci.4378-03.2004.

84. Ferrer, C., Hsieh, H., and Wollmuth, L.P. (2018). Input-specific maturation of NMDAR-mediated transmission onto parvalbumin-expressing interneurons in layers 2/3 of the visual cortex. J. Neurophysiol. *120*, 3063–3076. https://doi.org/10.1152/jn.00495.2018.

85. Han, K.S., Cooke, S.F., and Xu, W. (2017). Experience-Dependent Equilibration of AMPAR-Mediated Synaptic Transmission during the Critical Period. Cell Rep. *18*, 892–904. https://doi.org/10.1016/j.celrep.2016.12.084.

86. Wan, C., Xu, Y., Cen, B., Xia, Y., Yao, L., Zheng, Y., Zhao, J., He, S., and Chen, Y. (2021). Neuregulin1-ErbB4 Signaling in Spinal Cord Participates in Electroacupuncture Analgesia in Inflammatory Pain. Front. Neurosci. *15*, 636348. https://doi.org/10.3389/fnins.2021.636348.

87. Liu, S., Wang, Z.F., Su, Y.S., Ray, R.S., Jing, X.H., Wang, Y.Q., and Ma, Q. (2020). Somatotopic Organization and Intensity Dependence in Driving Distinct NPY-Expressing Sympathetic Pathways by Electroacupuncture. Neuron *108*, 436–450.e7. https://doi.org/10.1016/j.neuron.2020.07.015.

88. Lin, W., Li, Z., Liang, G., Zhou, R., Zheng, X., Tao, R., Huo, Q., Su, C., Li, M., Xu, N., et al. (2023). TNEA therapy promotes the autophagic degradation of NLRP3 inflammasome in a transgenic mouse model of Alzheimer's disease via TFEB/TFE3 activation. J. Neuroinflammation *20*, 21. https://doi.org/10.1186/s12974-023-02698-w.

89. Williamson, M.R., Fuertes, C.J.A., Dunn, A.K., Drew, M.R., and Jones, T.A. (2021). Reactive astrocytes facilitate vascular repair and remodeling after stroke. Cell Rep. *35*, 109048. https://doi.org/10.1016/j.celrep.2021.109048.

STAR★METHODS

KEY RESOURCES TABLE

REAGENT or RESOURCE	SOURCE	IDENTIFIER
Antibodies		
Rabbit anti-c-Fos	Cell Signaling Technology	Cat# 2250; RRID:AB_2247211
Rabbit anti-Parvalbumin	AbCam	Cat# ab11427; RRID:AB_298032
Rabbit anti-CaMKIIα	AbCam	Cat# ab181052; RRID:AB_2891241
Alexa Fluor 488-anti-Rabbit secondary antibody	AbCam	Cat# ab150113; RRID:AB_2576208
Alexa Fluor 594-anti-Rabbit secondary antibody	AbCam	Cat# ab150080; RRID:AB_2576208
DAPI	Thermo Fisher Scientific	Cat# D3571; RRID:AB_2307445
Rabbit polyclonal Antibody to GluN2A	Invitrogen	Cat# A-6473; RRID:AB_1501807
Rabbit polyclonal Antibody to GluN2B	Cell Signaling Technology	Cat# 4207; RRID:AB_1264223
HRP-conjugated secondary antibodies	Abbkine	Cat# A21020; RRID:AB_2876889
Bacterial and virus strains		
rAAV-CAMKIIα-GCaMP6s-WPRE-pA	BrainVTA	Cat# PT-0110
rAAV-CAG-DIO-GCaMP6s-WPRE-pA	BrainVTA	Cat# PT-0196
rAAV-CAMKIIα-hM4D(Gi)-EGFP-WPRE-pA	BrainVTA	Cat# PT-0524
rAAV-EF1a-DIO-hM4D(Gi)-EGFP-WPREs	BrainVTA	Cat# PT-0987
rAAV-EF1a-DIO-hM3D(Gq)-EGFP-WPREs	BrainVTA	Cat# PT-0988
rAAV-hSyn-EGFP-WPRE-pA	BrainVTA	Cat# PT-0241
rAAV-CAMKIIα-EGFP-WPRE-hGH pA	BrainVTA	Cat# PT-0290
rAAV-CAG-DIO-EGFP-WPRE-hGH pA	BrainVTA	Cat# PT-0168
rAAV-hSyn-iGluSnFR(A184S)-WPRE-hGH pA	BrainVTA	Cat# PT-1140
Chemicals, peptides, and recombinant proteins		
Clozapine-N-oxide (CNO)	Sigma-Aldrich	Cat# C0832
Cresyl violet	Sigma-Aldrich	Cat# 10510-54-0
Muscimol hydrobromide	Sigma-Aldrich	Cat# G019
Ro25	Sigma-Aldrich	Cat# HY-13993
TCN-201	Sigma-Aldrich	Cat# SML0416
QuickBlock Blocking Buffer	Beyotime	Cat# P0252
Experimental models: Organisms/strains		
Mouse: C57BL/6J	Guangzhou University of Chinese Medicine	N/A
Mouse: Pvalbtm1(cre)Arbr/J (PV-Cre)	Peking University	N/A
Mouse: Pvalb-tdTomato-Ai9 (PV-TD)	Peking University	N/A
Software and algorithms		
MATLAB 2019b	MathWorks	https://www.mathworks.com
GraphPad Prism 8.0	GraphPad Software	https://www.graphpad.com/scientific-software/
ImageJ – Fiji 2.0.0	Schneider et al.2012	https://imagej.nih.gov/ij/
R 4.1.3	The R Foundation	http://www.r-project.org/
Offline Sorter V 3.3.5	Plexon	https://plexon.com/products/offline-sorter
NeuroExplorer V 5	Nex Technologies	https://www.neuroexplorer.com
Other		
Optogenetic Fiber Optic Cannula	Newdoon	N/A

RESOURCE AVAILABILITY

Lead contact

Further information and requests for resources and reagents should be directed to and will be fulfilled by the lead contact, Lulu Yao (yaolulu@gzucm.edu.cn).

Materials availability

This study did not generate unique reagents.

Data and code availability

- All data generated in this study are available from the supplemental information or the Zenodo repository (https://doi.org/10.5281/zenodo.10863015).
- This paper does not report original code.
- Any additional information required to reanalysis the data reported in this paper is available from the lead contact upon request.

EXPERIMENTAL MODEL AND STUDY PARTICIPANT DETAILS

Animals and housing conditions

Male C57BL/6J mice (5-8 weeks old) were purchased from the Animal Laboratory Center of Guangzhou University of Chinese Medicine (Guangzhou, China). PV-Cre (Pvalbtm1(cre)Arbr/J) and PV-TD (Pvalb-tdTomato-Ai9) mouse lines were kind gifts from Q Zhou. Male mice (weighing 15–30 g) aged 6–12 weeks were used and housed with food and water *ad libitum* on a normal 12-h light–dark cycle (light on at 07:00 am) with temperature (20–25°C) and humidity (40–70%) precisely controlled. Experimental procedures were performed exclusively during the light phase. All experiments were carried out following the principles of the Basel Declaration and the National Institutes of Health Guide for Laboratory Animals, the ARRIVE guidelines. And Guangzhou University of Chinese Medicine Committee approving the experiments and confirming that all experiments conform to the relevant regulatory standards (approval *No.20200402013*). Mice were randomized into different groups: Sham+shamEA, Sham+EA, Stroke+shamEA, Stroke+EA (including different EA stimulation frequencies), fiber photometry, *in vivo* pharmacogenetic manipulations, multichannel electrophysiology and *in vitro* electrophysiological recording.

METHOD DETAILS

Photothrombotic model surgery procedures

Mice were deeply anesthetized with 3% isoflurane and maintained with intraperitoneal injection of 1.25% avertin solution (80 mg/kg). The photo-chemical stroke model has established at previously reported.[31,80] Briefly, after injecting Rose Bengal (RB) solution (10 mg/kg) into the abdominal cavity, a laser irradiation (530nm and 15mW) was performed in right M1FL (forelimb region of M1, coordinates: 0.74 mm anterior to Bregma, 1.5 mm lateral to midline, superficial) to create a local infarction. To confirm the ischemia of M1FL region, mice were monitored for Cortical cerebral blood with Laser Speckle Contrast Imaging system before and after surgery (The skull was exposed and recording was lasted for 2 min after photothrombotic model surgery procedures). The sham group underwent the same surgical procedure, except that they weren't performed to the laser.

Behavioral tests

Behavioral tests of all groups were conducted before and after photothrombotic model surgery, and after 1 day, 3 days and 7 days of EA/Sham EA stimulation.

Grid walking test

The apparatus consisted of a black elevated that was leveled grid with openings (with 15 mm * 15 mm grid squares), and it that was made of polyvinyl chloride. The mice were gently placed in the center. A camera recorded the routes of the mice as they moved for a period of 5 min. A foot fault was recorded when the affected forelimb paw fell from or slips off the rung. We then quantified foot fault index of the affected forelimb (foot faults/total steps * 100%) to assess the ability of the mouse forelimb locomotion.

Adhesive sticker removal test

This behavioral test was used to assess the ability of the mouse to perform sensorimotor tasks, and it consists of two quantifiable indicators, sensory score and motor score.[81] Specifically, we put an adhesive paper on the affected forelimb of the mouse and gently placed it in a transparent box. Two scores including sense score and the motor score were recorded during the test. First, we recorded the time taken for the mice to notice the adhesive paper on their affected forelimb paw (sensory score). Then we calculated the time taken for the mice to remove the adhesive paper from their affected forelimb paw (motor score). The mice were limited to a maximum of 30 s to notice the adhesive sticker and 90 s to remove it.

Forelimb grip strength test

The grasping power of mice forelimbs was measured by a Grip Tester. The protocol of this behavioral test was based on methods previously described.[80] Briefly, we placed the forelimbs of mice on the grip board, then grabbed their tails and pulled them diagonally rearward. Record the final grip strength value displayed by the Grip Tester. We then quantified grip strength value (average over each of three trials) to assess the ability of the mouse forelimb paw locomotion.

Virus injection

Mice were anaesthetized with avertinl (i.p, 80 mg/kg) before surgery, and placed in the stereotaxic frame. After disinfection with 1% Iodophor disinfectant, a small incision of the scalp was created to expose the skull. Then, 0.3% hydrogen peroxide was applied to clean the skull, and craniotomy was conducted. The viral injection coordinate of M1FL was: +0.74 mm anterior to Bregma, -1.5 mm lateral to midline, and −0.94 mm ventral to the cortical surface. Injections were performed using a microsyringe pump. A Micro controller was used to deliver the virus solution to the target areas at a rate of 20-30 nL/min (total 200-300nL). All subsequent experiments were performed at least 3 weeks after virus injection to allow sufficient time for transgene expression and animal recovery. All viruses mentioned in this article were packaged by BrainVTA.

Fiber photometry

For fiber photometry experiments were performed at least 3 weeks after GCaMP6s/iGluSnFR (200 nL) injection at unilateral M1FL. Optic fiber implantation was carried out immediately after virus injection. It was implanted unilaterally 0.1 mm more dorsal than virus injections, and fixed in head with dental cement and anchor screws. The implanted fiber was connected to Fiber Optic Meter through an optical fiber patch cord.[82] Calcium signals were recorded throughout the forelimb grip strength behavioral testing. Data were analyzed using MATLAB 2019b. Changes in fluorescence values ($\Delta F/F$) were calculated as (F-F0)/F0*100%.

In vivo pharmacogenetic manipulations

PV-Cre mice were injected with rAAV-EF1a-DIO-hM4D(Gi)-EGFP -WPREs (AAV-DIO-hM4Di) or rAAV-EF1a-DIO-hM3D(Gq)-EGFP -WPREs (AAV-DIO- hM3Dq) virus (300 nL) into the contralesional M1FL to inhibit/excite M1FL PV-neurons. WT mice were injected with rAAV-CaM-KIIα-hM4D(Gi)-EGFP -WPRE-pA (AAV-CaMKIIα-hM4Di) virus (300 nL) into the contralesional M1F Lto inhibit pyramidal neurons, and injected rAAV-hSyn-EGFP -WPRE-pA (AAV-control) into the contralesional M1FL as control. The location of virus expression was confirmed using immunofluorescence imaging on a confocal microscope (Leica, Germany). Mice received Clozapine-N-oxide (CNO) (i.p, 2 mg/kg; BrainVTA, dissolved in dimethylsulfoxide (DMSO) and sterile 0.9% saline) 30 min before behavioral conditioning or testing.

In vivo multichannel electrophysiology

Mice were anesthetized with isoflurane (induction 3%, maintenance 1.5%) and placed in the stereotaxic frame. Surgery was performed using the 'notouch' sterile procedure, and all surgical tools were sterilized prior to surgery. Animals were implanted with a custom-built electrodes above the M1FL nucleus (+0.74 mm anterior to Bregma, -1.5 mm lateral to midline, and −0.94 mm ventral to the cortical surface), which consisted of 8 individually insulated nichrome wires arranged in a 2*4+1 pattern (200 mm spacing between wires). Three screws were implanted to secure electrode array implants. Multi-wire electrodes were unilaterally implanted in the targeted brain regions. After surgery, mice were allowed to recover for 7 to 14 days. Neural signals were simultaneously recorded (16 bits, 30 kHz) from implanted 16-ch arrays using a Plexonl data acquisition system. Spikes were recorded for 5 minutes in each group. Spikes were sorted offline using Offlinesorter software. The final recording location was verified using histology after the electrolytic lesions (12 μA, 30 s).

Principal component analysis was then used to calculate the principal component score of the unsorted neuronal waveforms and scores were plotted in a three-dimensional principal component space. Waveforms with similar characteristics segregate into distinct clusters in the principal component spaces, and these clustered waveforms were defined as neuronal waveforms of a single neuron. Sorted spikes were further analyzed using NeuroExplorer (Nex Technologies, USA). The activity of interneurons (PV/fast-spiking-neurons) and pyramidal neurons (excitatory neurons) detected during electrophysiological recording *in vivo* was distinguished based on firing rate and waveform characteristics.[31]

In vitro electrophysiological recording

Mice were euthanized and the brain was quickly removed into the ice-cold cutting solution (aCSF), which containing (mM): 110 choline chloride, 25 D-glucose, 25 NaHCO$_3$, 11.6 sodium ascorbate, 2.5mM KCl, 7mM MgSO4, 3.1mM sodium pyruvate, 1.25 NaH$_2$PO$_4$, and 0.5 CaCl$_2$ and gassed with 95% O$_2$ and 5% CO$_2$.The left hemisphere of the brain was kept for further recording. Coronal frontal sections (400 μm) were cut on a VT1200S vibratome. The slices were firstly incubated in the aCSF at about 32°C for 30 min, and then transferred to the room temperature for at least 1h, and the aCSF contained (mM): 127 NaCl, 2.5 KCl, 1.25 NaH$_2$PO$_4$, 25mM NaHCO$_3$, 25 D-glucose, 2 CaCl$_2$, and 1 MgSO$_4$. The recorded neurons were located in the layer5/6 of M1.

To record the action potential and analyzed the intrinsic excitability, the current at a 20pA increment with 500 ms duration was injected to the recorded neurons at a current clamp-recording mode. The recording solution in the pipette contained (mM): 105 K-gluconate, 10 HEPES, 0.1 EGTA, 10 phosphocreatine, 4 ATP-Mg, 0.3 GTP-Na, 0.3EGTA, pH 7.3±0.1, 295 mosM±5. To confirm the effect of chemogenetic

inhibition of PV and CAMKIIα positive neurons, CNO (5mM) was perfused. To record mEPSCs, the neurons were clamped at -70 mV and bathed application with TTX (1μM). Patch pipette (resistance 4∼7 MΩ) was filled with solution containing as follows (mM): 125 CsMeSO₄, 5 NaCl, 1.1 EGTA, 10 HEPES, 0.3 Na₂GTP, 4 Mg-ATP, and 5 QX-314, pH 7.3±0.1, 295 mosM±5.[83] To obtain the AMPAR/NMDAR ratio PTX (100μM) was added to the recording solution, the stimulation electrode is placed on the same layer of the detected cell with a 40 μs pulse duration at 0.1 Hz. AMPAR-mediated EPSC was measured at -70mV, The NMDAR-mediated EPSCs was measured at +40mV, 50ms after current stimulation.[84] A Multiclamp 700B amplifier and Digidata 1550B (Molecular Devices, USA) were used to record and analyze the electrical activity of neurons, with a filtering frequency of 2 KHz and a sampling frequency of 10 KHz.[85]

EA stimulation treatment

Anesthesia was induced using 3% isoflurane, and maintained with 2% isoflurane using a mask. Mice were laid supine and fixed. Following routine sterilization of the scalp and neck, a concentric EA needle (φ 0.5 × 10 mm) was inserted at GV14 (Dazhui, between the 7th cervical vertebra and the 1st thoracic vertebra, in the middle of the back.) with needle angle 45° to a depth of 2 to 3 mm.[31] EA stimulation was performed with the electrical current of 1.0 mA, a pulse width of 1 ms and a frequency of 2 Hz, 50 Hz or 100 Hz for 20 min by using a Master-8 Eight Channel Programmable Pulse Generator (Master8) and 2 ISO-Flex stimulus isolators (AMPI).[86] The mice showed visible muscle contraction near the acupoint during stimulus.[12] EA stimulation was performed once per day starting after the day of stroke surgery for 7 times. Considering that insertion of acupuncture may exert the effect, in the shamEA group, mice were anesthetized for the same amount of time, but EA needle was not inserted.[87,88]

Histological assessment

Immunostainings were performed after 1D or 7D after stroke induction. After mice were euthanized through a pentobarbital sodium overdose and subsequently perfused with cold PBS followed by 4% paraformaldehyde (PFA) in PBS, their brains were frozen and sectioned coronally at 40-mm thickness using a sliding microtome. The primary antibodies used for fluorescent immunostaining were as follows: rabbit anti-c-Fos (1:500; Cell Signaling Technology,Cat# 2250), rabbit anti-Parvalbumin (1:1000; AbCam,Cat# ab11427), and rabbit anti-CAMKIIα (1:200;AbCam, Cat# ab181052). For fluorescen secondary antibodies, we used Alexa Fluor 488 goat anti-rabbit (1:500; AbCam, Cat# ab150080) and Alexa Fluor 488 goat anti-rabbit (1:500; AbCam, Cat# ab150113). Nissl staining was performed with 0.1% cresyl violet (Sigma-Aldrich,Cat# 10510-54-0) according to standard protocol in order to show the location of the electrodes. For cell number quantification, cells were counted from confocal image stacks using the optical dissector method counting.[89] Since there are few surviving neurons in the infarct core area, neurons located at the peri-infarcted zone instead of the infarted core in the ipsilateral(right) side were included to analyze (Figure S3B). The acquired images were processed and analyzed using ImageJ-Fiji or Adobe Photoshop software.

Western Blot

For western blot analysis, the M1FL tissues were collected and homogenized in a RIPA lysis buffer under deep anesthesia with Avertin. Protein concentrations were quantified by the Enhanced BCA Protein Assay Kit, and all samples were adjusted to 2 mg/mL. The extracted protein was boiled for 5 min at 95°C with 5 × loading buffer, and equal amounts of protein were separated via SDS–PAGE using a 10% SDS–PAGE gel and then were transferred to PVDF membranes at an appropriate voltage and duration. After blocking with QuickBlock blocking buffer for 15min at RT, the membranes were incubated with primary antibodies overnight at 4°C. Then, the membranes were incubated with goat anti-rabbit HRP-conjugated secondary antibodies (1:4000) for 1 h at room temperature after washing. Immunoblots were visualized with a chemiluminescence system, and quantified using FIJI software.

QUANTIFICATION AND STATISTICAL ANALYSIS

All data were analyzed using the appropriate statistical analysis methods with GraphPad Prism software, version 9.0 (GraphPad Software, Inc., USA), and the data are expressed as the *mean ± SEM*. Mice were randomly assigned to treatment conditions. Data were analysed blind whenever possible. No statistical methods were used to predetermine sample sizes. Sample sizes for all histochemical, cytokine and transmitter measurements were chosen according to recently reported studies. We conducted statistical comparisons between two groups using Student's *t* -tests. *Two-way analysis of variance (ANOVA)* and *Tukey* post hoc analyses were used in analyses with multiple experimental groups. And *one-way ANOVA* followed by *Tukey* hoc test was used in analyses with multiple groups at single time. Comparisons were two-tailed, and significance levels are indicated as *$P < 0.05$, **$P < 0.01$, ***$P < 0.001$, ****$P < 0.0001$ and not significant (n.s). *P* values are not provided as exact values when they less than 0.0001.